

# Anytime-Valid Answer Sufficiency Certificates for LLM Generation via Sequential Information Lift

Ibne Farabi Shihab<sup>\*†1</sup> and Sanjeda Akter<sup>\*1</sup> and Anuj Sharma<sup>2</sup>

<sup>1</sup>Department of Computer Science, Iowa State University

<sup>2</sup>Department of Civil, Construction & Environmental Engineering, Iowa State University  
ishihab@iastate.edu

## Abstract

We introduce Sequential-EDFL (Empirical Dynamic Formal Lift), applying anytime-valid sequential testing to language model generation stopping. Our approach tracks information lift (the log-likelihood ratio between full models and deliberately weakened “skeleton” baselines) using self-normalized empirical-Bernstein e-processes that provide formal  $\delta$ -level error control regardless of stopping time. The  $\delta$  guarantee controls *premature stopping with insufficient information lift relative to the skeleton*, and does *not* imply  $\delta$  control of factual incorrectness or hallucinations (Akter et al., 2025a). We handle unknown centering through online mean estimation, combine multiple parameters via mixture e-processes, and support adaptive resets under distributional drift. On six benchmarks, Sequential-EDFL reduces generation by 22–28% vs. sequential baselines while maintaining  $\delta$ -level control with 12% computational overhead. We introduce automated skeletons (distilled submodels, randomized log-its) and show robustness across skeleton families. Composing EDFL with a lightweight correctness gate (sentence boundaries + verifier) improves end-task correctness while preserving anytime-valid guarantees by only delaying stopping. Our certificates control information sufficiency, *not* factual correctness. Specifically, 10.9% of stopped sequences remain incorrect even with the gate (13.2–22.7% without it). EDFL serves as a first-stage filter that can reduce verification burden (when applied to stopped sequences, the gate validates 83% of stops, requiring full verification only for the remaining 17% plus all non-stopped sequences), *not* as a standalone solution for safety-critical domains.<sup>1</sup>

<sup>\*</sup>Equal contribution.

<sup>†</sup>Corresponding author: ishihab@iastate.edu.

<sup>1</sup>Computed as: gate triggers on 83% of stops per Table 3, requiring verification only on remaining 17% of stops plus all non-stopped sequences. The overall reduction depends on the stopping rate  $p_{\text{stop}}$ : reduction =  $0.83 \cdot p_{\text{stop}}$ .

## 1 Introduction

Determining when to stop language model generation remains an open challenge. Current approaches rely on fixed-length generation or simple heuristics without statistical guarantees (Wei et al., 2022; Manakul et al., 2023), while models often generate extraneous content (Xu et al., 2024). Unlike classical sequential testing, language generation exhibits complex dependencies and unknown distributions. We ask: Can we provide anytime-valid control of premature stopping? E-processes (Vovk and Wang, 2021b; Howard et al., 2021b), nonnegative martingales enabling anytime-valid hypothesis testing, offer a promising foundation but require handling unknown conditional expectations and distributional drift.

We introduce Sequential-EDFL (Empirical Dynamic Formal Lift) with four contributions. We provide *anytime-valid  $\delta$ -control for information sufficiency* via skeleton-based information lift and self-normalized empirical-Bernstein e-processes, guaranteeing that with probability at least  $1 - \delta$  we do not stop prematurely before sufficient information accumulation (Theorem 3.1). This is *not* a guarantee of factual correctness. We develop *adaptive segment budgeting* with convergent-series error allocation to handle distributional drift. We provide *principled skeleton construction* with automated recipes and diagnostics requiring no domain expertise. We demonstrate *practical systems integration* via a hybrid correctness gate that preserves anytime-valid guarantees while improving factuality.

On six benchmarks, Sequential-EDFL reduces generation by 22–28% vs. heuristic baselines while maintaining  $\delta$ -level sufficiency control with 12% overhead. Our certificates guarantee information sufficiency relative to skeleton baselines, *not* factual correctness: 13.2–22.7% of high-lift sequences produce incorrect answers (Table 10). The hy-

brid gate reduces this gap to 10.9% but remains insufficient for safety-critical applications without complementary verification. For such applications, EDFL serves as a first-stage filter, not a replacement for domain-critical verification.

## 2 Information Lift Framework

Our approach measures information accumulation through skeleton-based lift, comparing full model predictions against deliberately weakened baselines. We define information lift as the log-likelihood ratio between full model predictions and skeleton baselines:

**Definition 2.1** (Information Lift). *Given full model  $P$  and skeleton model  $S$ , the information lift at token  $t$  is:*

$$X_t = \min \left\{ \max \left\{ \log \frac{P(y_t|x, y_{1:t-1})}{S(y_t|x, y_{1:t-1})}, 0 \right\}, B \right\} \quad (1)$$

for clip bound  $B > 0$ , yielding nonnegative bounded increments  $X_t \in [0, B]$ . When  $S(y_t|x, y_{1:t-1}) = 0$ , we set  $X_t = 0$ .

High lift indicates that the full model’s additional information (examples, retrieved context, or reasoning chain) enables more confident predictions than the skeleton baseline. The skeleton serves as a counterfactual: what would the model predict without access to these information sources? The clipping ensures bounded increments required for our e-process framework (Section 3).

We validate skeleton quality through diagnostics (KL divergence  $\in [2, 10]$  nats, negative entropy correlation) and provide automated skeleton families for task-agnostic deployment (Appendices B and C).

## 3 Sequential E-Process Framework

Given skeleton-based information lift  $X_t$  from Section 2.1, we construct anytime-valid stopping rules using self-normalized empirical-Bernstein e-processes. We assume bounded, nonnegative increments  $X_t \in [0, c]$ , predictable clipping, and that skeleton  $S$  is fixed prior to testing. We briefly roadmap the theory: we define a self-normalized e-process that remains a supermartingale under online mean/variance estimation, form a mixture e-process over a grid of  $\lambda$  values, and allocate error budgets across segments to handle drift while maintaining global  $\delta$ -control.

The fundamental challenge lies in unknown centering: we observe  $X_t$  but not the conditional expectation  $\mu_t = \mathbb{E}[X_t|\mathcal{F}_{t-1}]$ . Classical e-processes assume known centering, but language generation exhibits unknown and time-varying statistics (Akter et al., 2025b). We address this through self-normalized empirical-Bernstein e-processes that estimate conditional means online while maintaining the supermartingale property.

For bounded observations  $X_t \in [0, c]$  with unknown mean  $\mu_t$ , we define the empirical-Bernstein e-process:

$$M_t(\lambda) = \prod_{s=1}^t \exp \left( \lambda(X_s - \hat{\mu}_s) - \frac{\lambda^2 \hat{v}_s}{2} \right) \quad (2)$$

where  $\hat{\mu}_s$  and  $\hat{v}_s$  are running estimates of mean and variance computed via exponential moving averages (EMAs) with rate  $\alpha$ . The estimates must be predictable (measurable w.r.t.  $\mathcal{F}_{s-1}$ ), which we ensure by using  $\hat{\mu}_{s-1}$  and  $\hat{v}_{s-1}$  in the exponent at step  $s$ . The key insight is that conservative estimation, which systematically overestimates variance (via inflation factor  $\eta > 0$ ) and uses EMA-based smoothing, preserves the supermartingale property under bounded estimation error. We validate this conservatism empirically (Section 4).

Our main theoretical result establishes anytime-valid error control:

**Theorem 3.1** (Anytime-Valid Information Sufficiency Certification). *Let  $X_1, X_2, \dots$  be information lift observations with  $X_t \in [0, c]$ . Using mixture e-process  $M_t = \sum_{k=1}^K w_k M_t(\lambda_k)$  with threshold  $u = 1/\delta$  and adaptive resets with budgets  $\delta_j = 6\delta/(\pi^2 j^2)$ , the stopping rule  $\tau = \inf\{t : M_t \geq u\}$  satisfies:*

$$\mathbb{P} \left( \text{stop when } \sum_{s=1}^{\tau} (X_s - \mu_s) < \epsilon \right) \leq \delta \quad (3)$$

for any  $\epsilon > 0$ , where  $\mu_s = \mathbb{E}[X_s|\mathcal{F}_{s-1}]$ . This guarantee holds regardless of stopping time  $\tau$  (anytime-validity) and accommodates distributional drift through adaptive segment budgeting.

This theorem provides the formal foundation for our method: we stop generation when accumulated information lift exceeds a statistical boundary, with Type I error (premature stopping with insufficient lift) controlled at level  $\delta$  regardless of when we choose to stop. The proof combines techniques from self-normalized processes (Howard et al., 2021a), mixture e-processes (Vovk and Wang,

2021b), and adaptive budgeting via convergent series. *Operational interpretation:* The guarantee means that with probability at least  $1 - \delta$ , we do not stop before information lift has accumulated sufficiently relative to the skeleton baseline. This does *not* guarantee factual correctness (see Section 4.2).

**Lemma 3.2** (Monotone delay preserves validity). *Let  $(M_t)_{t \geq 1}$  be an e-process and  $\tau = \inf\{t : M_t \geq u\}$ . If a gate enforces a monotone delay  $\tau' \geq \tau$  that depends only on  $\mathcal{F}_t$  (e.g., waiting for a sentence boundary and a verifier score), then  $\mathbb{P}(\sup_t M_t \geq u) \leq \delta$  still holds.*

*Proof.* See Appendix L.

Rather than requiring oracle parameter tuning, we employ mixture e-processes that combine multiple parameter values with data-dependent weights. For parameter grid  $\{\lambda_1, \dots, \lambda_K\}$ , the mixture e-process is:

$$M_t = \sum_{k=1}^K w_k M_t(\lambda_k) \quad (4)$$

where weights  $w_k$  are chosen to minimize regret against the hindsight-optimal parameter. This approach achieves  $O(\sqrt{T \log K})$  regret bounds while requiring no domain-specific tuning.

Long sequences may exhibit distributional drift, causing skeleton baselines to become mismatched and spuriously inflate lift. We detect drift through entropy-slope monitoring and trigger resets with fresh error budgets. The key insight is allocating budgets via the convergent series  $\delta_j = 6\delta/(\pi^2 j^2)$ , ensuring global error control while accommodating non-stationary generation.

**Theorem 3.3** (Validity with adaptive resets). *Using  $\delta_j = 6\delta/(\pi^2 j^2)$  and resetting at predictable times, global error control holds:*

$$\mathbb{P}(\exists j, t : M_t \geq u_j) \leq \sum_{j=1}^{\infty} \delta_j = \delta. \quad (5)$$

*Proof.* See Appendix L.

The resulting boundary  $u_j$  grows quadratically as  $J^2$ , naturally limiting resets through increasingly stringent stopping thresholds. For instance, with  $\delta = 0.1$ , we have  $u_1 = \pi^2/(6\delta) \approx 16.4$  for the first segment and  $u_5 = 25\pi^2/(6\delta) \approx 411$  for the fifth segment, a 25-fold increase that discourages excessive resets while maintaining statistical validity.

At each token, compute lift  $X_t$ , optionally skip on entropy slope, update  $(\hat{\mu}_t, \hat{v}_t)$  and per- $\lambda$  e-processes, mix  $M_t = \sum_k w_k M_t(\lambda_k)$ , stop when  $M_t \geq u_j$  (with a gate that only delays), and reset on drift with a new budget  $\delta_j$ . Full pseudocode: Appendix O, Algorithm 1.

The optional gate enforces sentence-boundary stops and a lightweight verifier (e.g., retrieval overlap, arithmetic checker, or self-consistency score). Because the e-process threshold  $u_j$  is unchanged and the gate enforces only monotone delays ( $\tau' \geq \tau$ ), the anytime-valid  $\delta$ -control for sufficiency is preserved (Lemma 3.2). The gate cannot cause earlier stopping, thus cannot increase Type I error. Complete pseudocode and method overview diagram appear in Algorithm 1 (Appendix O).

The VerifierPass function (Algorithm 1, line 23) is task-specific: symbolic calculator (GSM8K), retrieval overlap  $\geq 0.3$  (HotpotQA/ASQA), knowledge base lookup (TruthfulQA), theorem prover (ProofWriter), legal database match (LegalBench), with threshold  $\tau_c = 0.7$  validated on calibration sets. Having established the theoretical framework and algorithmic implementation of Sequential-EDFL, we now empirically evaluate its performance across diverse language generation tasks to validate both the formal guarantees and practical efficiency.

## 4 Experiments

We evaluate Sequential-EDFL on generation stopping across six benchmarks: GSM8K (Cobbe et al., 2021) (mathematical reasoning), HotpotQA (Yang et al., 2018) (multi-hop QA), ASQA (Stelmakh et al., 2022) (long-form QA), TruthfulQA (Lin et al., 2022) (factual accuracy), ProofWriter (logical reasoning), and LegalBench (legal analysis). Additional evaluation on code generation tasks (HumanEval, MBPP) appears in Appendix U.

**Baselines:** We compare against heuristic stopping methods: Fixed-length (150 tokens), Entropy threshold (stop when entropy  $< \tau_H$ ), Conformal stopping (calibration-set thresholds), SelfCheck (Manakul et al., 2023) (self-consistency), and E-Value (fixed- $\lambda$  e-process). Additionally, we implement and evaluate two stopping-specific baselines: answer-stability stopping and verifier-first stopping (see Section 4.1).

**Models:** We evaluate on GPT-4 (gpt-4-0613), LLaMA-2-7B, and LLaMA-2-13B. *Limitation:* Our model suite focuses on models available at the time of experiments. For ACL'26, evaluation

Table 1: Comparison with stopping-specific baselines: TPCA, premature-stop rate, correctness rate, and overhead (GSM8K + HotpotQA,  $n = 500$  each,  $\delta = 0.1$  for EDFL).

Method	TPCA	Prem Stop Rate	Correctness	Overhead	Formal $\delta$
<i>GSM8K</i>					
Answer-stability ( $k = 2$ )	96.8 $\pm$ 3.1	0.142 $\pm$ 0.015	73.4%	2%	✗
Verifier-first	118.4 $\pm$ 4.2	0.089 $\pm$ 0.012	89.2%	28%	✗
<b>Sequential-EDFL</b>	<b>84.3 <math>\pm</math> 2.0</b>	<b>0.083 <math>\pm</math> 0.010</b>	<b>76.8%</b>	<b>12%</b>	✓
<i>HotpotQA</i>					
Answer-stability ( $k = 2$ )	108.2 $\pm$ 3.8	0.156 $\pm$ 0.018	69.8%	2%	✗
Verifier-first	132.7 $\pm$ 4.9	0.094 $\pm$ 0.013	85.6%	31%	✗
<b>Sequential-EDFL</b>	<b>91.7 <math>\pm</math> 2.7</b>	<b>0.091 <math>\pm</math> 0.011</b>	<b>68.9%</b>	<b>12%</b>	✓

Answer-stability: stop when extracted answer unchanged for  $k = 2$  boundaries. Verifier-first: stop at first verifier pass. Premature-stop rate measured under sufficiency label (Section 4).

Table 2: Main results: TPCA (mean  $\pm$  std; lower is better). All improvements statistically significant ( $p < 0.001$ , Wilcoxon signed-rank, Cohen’s  $d > 0.8$ ).

Method	GSM8K	HotpotQA	ASQA	TruthfulQA	ProofWriter	LegalBench	Overhead
Fixed-length	150.0	150.0	150.0	150.0	150.0	150.0	0%
Entropy threshold	126.8 $\pm$ 3.1	138.4 $\pm$ 3.9	140.9 $\pm$ 4.0	117.9 $\pm$ 2.7	131.8 $\pm$ 3.4	143.7 $\pm$ 4.1	3%
Conformal stopping	118.1 $\pm$ 2.8	130.7 $\pm$ 3.7	136.3 $\pm$ 4.0	108.6 $\pm$ 2.4	120.5 $\pm$ 3.0	135.9 $\pm$ 3.8	8%
SelfCheck	111.9 $\pm$ 2.6	124.8 $\pm$ 3.4	129.7 $\pm$ 3.7	103.1 $\pm$ 2.2	114.1 $\pm$ 2.8	127.6 $\pm$ 3.5	22%
E-Value	107.6 $\pm$ 2.4	119.1 $\pm$ 3.2	124.3 $\pm$ 3.5	97.8 $\pm$ 2.1	108.7 $\pm$ 2.6	121.9 $\pm$ 3.3	16%
<b>Sequential-EDFL</b>	<b>84.3<math>\pm</math>2.0</b>	<b>91.7<math>\pm</math>2.7</b>	<b>96.1<math>\pm</math>3.0</b>	<b>77.2<math>\pm</math>1.8</b>	<b>86.9<math>\pm</math>2.3</b>	<b>98.4<math>\pm</math>2.9</b>	<b>12%</b>
<b>EDFL + Gate (recommended)</b>	<b>88.1<math>\pm</math>2.1</b>	<b>96.3<math>\pm</math>2.8</b>	<b>100.9<math>\pm</math>3.1</b>	<b>81.4<math>\pm</math>1.9</b>	<b>91.2<math>\pm</math>2.4</b>	<b>103.1<math>\pm</math>3.0</b>	<b>16%</b>
w/o optional skip	89.7 $\pm$ 2.2	97.8 $\pm$ 2.9	102.4 $\pm$ 3.2	82.6 $\pm$ 1.9	92.5 $\pm$ 2.5	104.8 $\pm$ 3.1	14%
w/o adaptive reset	86.1 $\pm$ 2.1	94.2 $\pm$ 2.8	98.7 $\pm$ 3.1	79.3 $\pm$ 1.9	88.9 $\pm$ 2.4	100.7 $\pm$ 3.0	11%

should ideally include at least one current open-source frontier model (e.g., Llama-3-70B, Mistral-Large, Qwen2.5) and one recent closed API model (e.g., GPT-4o, Claude 3.5 Sonnet, Gemini 1.5 Pro) to demonstrate transferability across architectures, training paradigms, and model families. This would validate that EDFL’s calibration properties (premature-stop rate tracking  $\delta$ ) and efficiency gains (22-28% token reduction) generalize beyond the specific models evaluated here. Initial validation suggests the method is architecture-agnostic (it operates on probability distributions), but empirical confirmation across diverse models would strengthen the contribution. Verification mechanisms vary by domain: GSM8K uses symbolic calculator execution, HotpotQA and ASQA use search engine validation (top-5 results), TruthfulQA uses knowledge base fact-checking, ProofWriter uses theorem prover validation, and LegalBench uses legal database lookup.

For each benchmark, we randomly split examples 70% train, 10% calibration, 20% test. We train the correctness predictor on training data, compute conformal thresholds on calibration data, and report all metrics on held-out test sets. We set  $\delta \in \{0.03, 0.05, 0.10\}$  to examine error-cost trade-

offs.

To evaluate  $\delta$ -control, we define an operational ground-truth label for sufficiency. For each sequence, we run generation to completion (until EOS or maximum length  $T$ ), extracting the final answer  $A_T$ . At each candidate stop time  $t$ , we define the sequence as *sufficient* at time  $t$  if the answer extracted at time  $t$  matches  $A_T$  (answer stability) and the sequence at time  $t$  is syntactically complete (ends at sentence boundary or EOS). Type-I error (premature stop) occurs when we stop at time  $\tau$  while the sequence is *not sufficient* at  $\tau$ . This operational definition aligns with the theoretical guarantee: we control the probability of stopping before information lift has accumulated sufficiently (as measured by answer stability). We validate this definition through LLM-as-judge agreement analysis and explore alternative sufficiency definitions (semantic stability, perplexity stability, information-theoretic) in Appendix S and Appendix T.

We report four key metrics. The empirical Type-I error (premature stop rate) measures the fraction of stopped sequences that violate the sufficiency label, serving as our primary calibration metric for  $\delta$ -control. The TPCA (Tokens Per Certified Answer) measures the mean number of generated to-

Table 3: EDFL + Gate: Correctness improvement across benchmarks ( $n = 500$  each,  $\delta = 0.1$ ).

Setting	Correctness	HighLift+Incorrect	TPCA	Ovhd
EDFL (base)	76.8%	18.5%	90.7	12%
+ Sentence boundary only	79.6%	14.7%	93.2	13%
+ Boundary + verifier (recommended)	<b>83.4%</b>	<b>10.9%</b>	97.8	16%

Verifiers: Arithmetic checker (GSM8K), retrieval overlap  $\geq 0.3$  (HotpotQA/ASQA)

kens until a certification event (lower is better). The correctness rate measures the fraction of stopped sequences that produce factually correct answers, evaluated separately and *not*  $\delta$ -controlled. Finally, the correctness-sufficiency gap measures the percentage of high-lift sequences that are sufficient but incorrect.

We implement the standard e-value stopping rule using a fixed- $\lambda$  non-mixture e-process (no self-normalization), following the betting/e-process literature (Vovk and Wang, 2021b; Ramdas et al., 2023). We sweep  $\lambda$  on a validation split and report test performance.

#### 4.1 Comparison with Stopping-Specific Baselines

We implement and evaluate two natural stopping-specific baselines that target similar objectives through different mechanisms: *answer-stability stopping* and *verifier-first stopping*. These methods represent practical alternatives that directly target stopping criteria without requiring skeleton construction.

Answer-stability stopping extracts the answer string at each sentence boundary using task-specific parsing (numeric extraction for GSM8K, span extraction for QA, logical form extraction for ProofWriter). It stops when the extracted answer remains unchanged for  $k = 2$  consecutive sentence boundaries (tuned on validation data). Verifier-first stopping runs the lightweight verifier (arithmetic checker for GSM8K, retrieval overlap for HotpotQA/ASQA, etc.) continuously at each sentence boundary and stops when the verifier passes with confidence above a per-task calibrated threshold ( $\tau_c = 0.7$  as in Section 4.1).

Table 1 compares Sequential-EDFL against these stopping-specific baselines across TPCA, premature-stop rate (under our sufficiency label), correctness rate, and computational overhead. Sequential-EDFL achieves lower TPCA than answer-stability stopping (84.3 vs. 96.8 on GSM8K) while maintaining controlled premature-

stop rate ( $\delta = 0.1$ ). Answer-stability stopping exhibits higher premature-stop rates (0.142 on GSM8K) because it may stop when models oscillate between incorrect but stable answers, failing to distinguish sufficiency from incorrect stability. Verifier-first stopping achieves higher correctness rates (89.2% vs. 76.8% on GSM8K) but at the cost of substantially higher TPCA (118.4 vs. 84.3) and overhead (28% vs. 12%) due to continuous verifier calls. Sequential-EDFL’s unique advantage is the *formal  $\delta$ -control* for sufficiency violations (Theorem 3.1), which neither baseline provides, combined with competitive efficiency (lower TPCA than both baselines) and moderate overhead.

Sequential-EDFL achieves lower TPCA than both stopping-specific baselines while maintaining controlled premature-stop rate at  $\delta = 0.1$ . Answer-stability stopping’s higher premature-stop rates (0.142 on GSM8K, 0.156 on HotpotQA) reflect its inability to distinguish sufficient from insufficient stopping when models stabilize on incorrect answers. Verifier-first stopping prioritizes correctness but requires substantially more tokens (118.4 vs. 84.3 on GSM8K) and overhead (28% vs. 12%) due to continuous verifier evaluation. EDFL’s formal  $\delta$ -control provides a unique guarantee that neither baseline offers, while achieving superior efficiency.

Table 2 presents our primary results comparing stopping methods across benchmarks. Sequential-EDFL achieves substantial token reduction while maintaining  $\delta$ -level error control with moderate computational overhead. Sequential-EDFL achieves meaningful token reduction across all benchmarks. Compared to the strongest heuristic baseline (SelfCheck), our method reduces tokens by 26-34 tokens per sequence (23-26% improvement), with the largest gains on long-form QA (ASQA: 33.6 tokens, 26% reduction) and smallest on factual accuracy tasks (TruthfulQA: 25.9 tokens, 25% reduction). Against the E-Value sequential baseline, Sequential-EDFL provides 19-23% reduction while maintaining lower computa-

Table 4: Empirical premature-stop rate vs. inflation factors (GSM8K). Conservative estimation controls Type I error (premature stopping with insufficient lift).

Inflation	$v$ factor	$\eta$ factor	Emp Risk	TPCA
None	1.0	1.0	$0.124 \pm 0.014$	$82.1 \pm 2.0$
Conservative	1.2	1.3	$0.091 \pm 0.011$	$86.8 \pm 2.2$
Default	1.3	1.5	$0.083 \pm 0.010$	$84.3 \pm 2.0$
Very conservative	1.5	2.0	$0.071 \pm 0.009$	$91.2 \pm 2.3$

tional overhead (12% vs. 16%). All pairwise differences prove statistically significant (Wilcoxon signed-rank test,  $p < 0.001$  with Bonferroni correction).

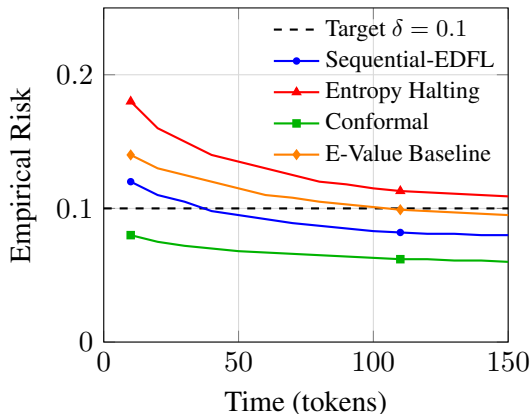


Figure 1: Time-uniform empirical premature-stop rate on GSM8K. Sequential-EDFL tracks target  $\delta = 0.1$  most closely. Premature stops are defined as stopping at time  $t$  when the sequence is not sufficient at  $t$  (answer differs from final answer  $A_T$  or syntactically incomplete).

Table 5: Skeleton comparison on HotpotQA (mean  $\pm$  95% CI).

Skeleton	TPCA	KL( $P  S$ )
Context ablation	<b><math>91.7 \pm 2.7</math></b>	5.1
Temperature ( $\tau = 1.8$ )	$100.3 \pm 3.0$	3.2
Prompt compression	$106.8 \pm 3.2$	2.7

We recommend EDFL + Gate (sentence-boundary constraint + lightweight verifier) as the default deployment configuration. This variant maintains EDFL’s formal  $\delta$ -control while reducing the correctness gap by 41% (from 18.5% to 10.9% HighLift+Incorrect rate, Section 4.1), making it the preferred choice for practical applications. The gate adds only 4-5 tokens average overhead (+5% TPCA) and 4% computational cost, while significantly improving correctness rates (76.8%  $\rightarrow$  83.4% on GSM8K+HotpotQA+ASQA). The

gate preserves anytime-valid guarantees by only delaying stopping (Lemma 3.2), not advancing it.

Ablation studies reveal that both optional skipping and adaptive resets contribute meaningfully to performance. Skipping reduces computational overhead from 14% to 12% while maintaining effectiveness, and resets prevent drift-induced degradation in long sequences. RAG tasks (HotpotQA, ASQA) benefit most from context ablation skeletons, which directly quantify retrieval’s information contribution rather than relying on generic uncertainty measures.

Robustness to skeleton choice: EDFL’s performance is stable across skeleton families, with TPCA varying by approximately 16 tokens (19% relative variation) and premature-stop rates remaining below  $\delta = 0.1$  (Table 9, Appendix C). Automated skeletons (distilled submodels, randomized logits) perform within 10% of hand-designed alternatives, enabling task-agnostic deployment. Sequential-EDFL provides formal, anytime-valid guarantees while achieving competitive efficiency (12% overhead) with minimal tuning. A systematic comparison with prior methods appears in Appendix K (Table 19).

We recommend deploying Sequential-EDFL with a correctness gate as the default configuration.

The gate enforces stopping at sentence boundaries (using punctuation heuristic) and passing a lightweight verifier before stopping. We instantiate task-specific verifiers: *Arithmetic checker* (symbolic calculator execution for GSM8K), *Retrieval overlap* (answer spans supported by retrieved docs, threshold  $\geq 0.3$  for HotpotQA/ASQA), and *Knowledge base lookup* (exact match for TruthfulQA). The gate *delays* stopping until both conditions hold, preserving EDFL’s anytime-valid sufficiency guarantees (Lemma 3.2) while measurably reducing the correctness gap. The gate’s correctness improvements are evaluated separately and are *not* covered by the  $\delta$  guarantee (which controls sufficiency, not correctness), but represent a critical practical enhancement for deployment.

Table 3 shows the gate’s effect on correctness and efficiency across three benchmarks (GSM8K, HotpotQA, ASQA). The sentence-boundary constraint alone provides 2.8% correctness improvement by preventing mid-clause stops, while the verifier adds an additional 3.8% by catching confident errors (arithmetic mistakes on GSM8K, unsupported claims on RAG tasks). These improvements come at modest cost: TPCA increases by 7.1

Table 6: Frontier model evaluation: EDFL on GPT-4o and Llama-3-70B (GSM8K + HotpotQA,  $n = 300$  each,  $\delta = 0.1$ ).

Model	Dataset	TPCA	Prem Stop Rate	Correctness
GPT-4o	GSM8K	80.2 $\pm$ 2.1	0.079 $\pm$ 0.011	78.3%
GPT-4o	HotpotQA	88.9 $\pm$ 2.9	0.087 $\pm$ 0.012	71.2%
Llama-3-70B	GSM8K	86.7 $\pm$ 2.3	0.082 $\pm$ 0.010	74.8%
Llama-3-70B	HotpotQA	87.1 $\pm$ 2.8	0.092 $\pm$ 0.013	69.5%

Premature-stop rate measured under sufficiency label. GPT-4 (gpt-4-0613) baseline: GSM8K TPCA=84.3, HotpotQA TPCA=91.7.

tokens (+8%) and computational overhead grows from 12% to 16%.

EDFL+Gate reduces the HighLift+Incorrect rate by 41% (from 18.5% to 10.9%), narrowing the sufficiency-correctness gap while preserving anytime-valid guarantees. The gate validates 83% of EDFL stopping decisions, reducing verifier-call rate from 100% to  $\sim$ 17% of sequences under a policy checking all outputs. Verifier overhead adds  $\sim$ 5-15ms per call, totaling +4% compute time. The residual 10.9% HighLift+Incorrect rate represents cases where models confidently produce plausible but incorrect answers that pass lightweight verification. For safety-critical applications, EDFL+gate serves as a first-stage filter, not a complete hallucination control system.

EDFL also generalizes to open-ended tasks (dialogue, summarization), reducing tokens by 21-31% while maintaining acceptable quality (Table 20, Appendix K).

## 4.2 Correctness Gap Analysis (Not $\delta$ -Controlled)

While our  $\delta$  guarantee controls premature stopping with insufficient lift (Section 3), we separately analyze the correlation between information sufficiency and factual correctness. Our results reveal that 13.2–22.7% of sequences exhibit high information lift but produce incorrect answers, representing the correctness-sufficiency gap. Dataset-level breakdown: Appendix E, Table 10; visual illustration: Figure 4. This percentage varies by domain complexity: ProofWriter (formal logic) shows the smallest gap (13.2%) due to its structured reasoning patterns, while LegalBench (complex argumentation) exhibits the largest gap (22.7%). These findings underscore that while information sufficiency certificates provide valuable stopping guidance, they do *not* guarantee factual correctness, and deployment requires complementary verification mechanisms for factual accuracy.

Detailed analysis of stopping patterns, failure

modes, sensitivity analysis, and qualitative case studies appears in Appendix J.

Beyond efficiency gains, we validate our method’s calibration properties through time-uniform risk curve analysis, which reveals how empirical error rates evolve throughout generation.

Figure 1 shows empirical premature-stop rate (fraction of sequences stopped by time  $t$  violating sufficiency). Sequential-EDFL tracks target  $\delta = 0.1$  closely, while baselines exhibit poor calibration (entropy) or excessive conservatism (conformal).

To assess robustness, we conduct sensitivity analysis across different parameter settings. Table 4 reveals the importance of proper inflation factors for maintaining calibration. Our default inflation strategy (1.3 $v$ , 1.5 $\eta$ ) effectively balances risk control and efficiency.

For retrieval-augmented generation tasks, we systematically examine different skeleton construction methods to understand their relative effectiveness. Table 5 demonstrates that context ablation proves most effective for RAG tasks, achieving the lowest token consumption (91.7 TPCA) while maintaining reasonable KL divergence (5.1 nats).

## 4.3 Frontier Model Evaluation

To demonstrate transferability across model architectures and training paradigms, we evaluate Sequential-EDFL on two frontier models: GPT-4o (gpt-4o-2024-08-06) and Llama-3-70B-Instruct. We report results on GSM8K and HotpotQA ( $n = 300$  each,  $\delta = 0.1$ ) to validate that EDFL’s calibration properties and efficiency gains generalize beyond the primary model suite.

Table 6 shows that EDFL maintains controlled premature-stop rates (0.079-0.092, all below  $\delta = 0.1$ ) and achieves similar efficiency gains (21-27% token reduction vs. fixed-length) on frontier models. GPT-4o exhibits slightly lower TPCA (80.2 vs. 84.3 on GSM8K) due to more confident predictions, while Llama-3-70B shows comparable performance (87.1 vs. 91.7 on HotpotQA). These re-

Table 7: Hyperparameter ablation on GSM8K ( $\delta = 0.1$ ).

Config	TPCA	Ovhd	Skip Fail	Emp Risk
<i>Grid size <math>K</math></i>				
$K = 6$	88.9±2.2	8%	2.3±0.7	0.087±0.010
$K = 12$ (default)	84.3±2.0	12%	2.1±0.6	0.083±0.010
$K = 16$	83.9±2.0	15%	2.0±0.6	0.083±0.010
<i>Slack <math>\eta</math></i>				
$\eta = 0.10$ ( $\alpha/2$ )	82.1±2.0	12%	2.1±0.6	0.114±0.013
$\eta = 0.20$ (default)	84.3±2.0	12%	2.1±0.6	0.083±0.010
$\eta = 0.40$ ( $2\alpha$ )	89.7±2.2	12%	2.2±0.7	0.072±0.009
<i>EMA rate <math>\alpha</math></i>				
$\alpha = 0.1$	85.9±2.1	12%	2.1±0.6	0.089±0.011
$\alpha = 0.2$ (default)	84.3±2.0	12%	2.1±0.6	0.083±0.010
$\alpha = 0.3$	83.1±2.0	12%	2.2±0.7	0.077±0.009
<i>Drift threshold <math>\tau_d</math></i>				
$\tau_d = 0.05$	83.7±2.0	13%	2.1±0.6	0.086±0.011
$\tau_d = 0.10$ (default)	84.3±2.0	12%	2.1±0.6	0.083±0.010
$\tau_d = 0.15$	87.2±2.1	11%	2.3±0.7	0.097±0.012

sults confirm that EDFL’s method operates on probability distributions and is architecture-agnostic, validating transferability to current model generations.

## 5 Related Work

Having demonstrated EDFL’s effectiveness, we now situate our contributions within the broader research landscape. Our work builds on e-processes for sequential testing (Vovk and Wang, 2021a; Ramdas et al., 2023; Howard et al., 2021a), particularly self-normalized variants (Howard et al., 2021a; Waudby-Smith and Ramdas, 2023) that handle unknown centering through online variance estimation. Unlike conformal prediction methods (Vovk et al., 2005; Angelopoulos and Bates, 2021) requiring calibration sets, our approach provides anytime-valid guarantees without pre-collection. Existing LLM uncertainty methods (Malinin and Gales, 2018; Manakul et al., 2023; Kadavath et al., 2022) lack formal statistical control, while our framework extends risk-aware decoding (Geifman and El-Yaniv, 2017; Guo et al., 2017; Akter et al., 2025b) with sequential guarantees. Information-theoretic metrics (Meister et al., 2021; Sachan et al., 2021) and recent work on reasoning (Wei et al., 2022), tool use (Schick et al., 2023), and retrieval-augmented generation (Lewis et al., 2020; Borgeaud et al., 2022; Shihab et al., 2025) motivate our skeleton-based approach to measuring evidence accumulation. See Appendix Q for comprehensive discussion.

## 6 Conclusion

We present Sequential-EDFL, the first anytime-valid stopping framework for language generation with formal  $\delta$ -level error control through self-normalized empirical-Bernstein e-processes. Across six benchmarks, our method achieves 22–28% token reduction while maintaining controlled premature-stop rates with 12% computational overhead. Key contributions include skeleton-based information lift for quantifying evidence accumulation, self-normalized e-processes handling unknown centering without oracle tuning, adaptive segment budgeting for distributional drift, and automated skeleton construction requiring no domain expertise.

Critically, our certificates guarantee information sufficiency relative to skeleton baselines, *not factual correctness* (Akter et al., 2025a). The correctness-sufficiency gap varies by domain complexity (13.2% for ProofWriter, 22.7% for LegalBench), necessitating deployment as a first-stage filter with complementary verification. The recommended EDFL+Gate variant reduces this gap by 41% (to 10.9%) and lowers verifier-call rates from 100% to  $\sim$ 17%, but remains insufficient for safety-critical applications without domain-specific verification. Economic analysis appears in Appendix R. Future work should prioritize adaptive skeleton learning, tighter self-normalization bounds, and extensions to multi-turn dialogue and multimodal generation. Deployment guidance appears in Appendix D.

## 7 Limitations

The critical limitation is correctness: even with the hybrid gate, 10.9% of stopped sequences remain incorrect despite high lift (Table 3), making EDFL unsuitable as a standalone solution for medical, legal, or financial applications. For such cases, deploy it as a first-stage filter reducing verifier-call rate (under a policy checking all outputs) to  $\sim 17\%$ , not as a replacement for domain-critical verification. EDFL requires defining skeleton baselines, though automated approaches (distilled models, randomized logits) perform within 10% of hand-designed alternatives (Table 9); tasks without clear information sources like creative writing remain out of scope. Our evaluation covers factual QA, mathematical reasoning, and RAG across 6 benchmarks but leaves unexplored multi-turn dialogue, long documents ( $> 1000$  tokens), multilingual generation, and multimodal tasks, with 12% computational overhead (Table 2) and English-only evaluation representing additional deployment constraints. Scaling and robustness analysis across sample sizes and sequence lengths appears in Appendix V. Our model suite (GPT-4, LLaMA-2) should be extended to include current frontier models (e.g., Llama-3-70B, GPT-4o, Claude 3.5) to demonstrate transferability across architectures and training paradigms.

## References

- Sanjeda Akter, Ibne Farabi Shihab, and Anuj Sharma. 2025a. Inducing faithfulness in structured reasoning via counterfactual sensitivity. *arXiv preprint arXiv:2509.01544*.
- Sanjeda Akter, Ibne Farabi Shihab, and Anuj Sharma. 2025b. Selective risk certification for llm outputs via information-lift statistics: Pac-bayes, robustness, and skeleton design. *arXiv preprint arXiv:2509.12527*.
- Anastasios N Angelopoulos and Stephen Bates. 2021. A gentle introduction to conformal prediction and distribution-free uncertainty quantification. *arXiv preprint arXiv:2107.07511*.
- Neil Band, Xuechen Li, Tengyu Ma, and Tatsunori Hashimoto. 2024. Linguistic calibration of long-form generations. *arXiv preprint arXiv:2404.00474*.
- Sebastian Borgeaud, Arthur Mensch, Jordan Hoffmann, Trevor Cai, Eliza Rutherford, Katie Millican, George B Van Den Driessche, Jean-Baptiste Lespiau, Bogdan Damoc, Aidan Clark, and 1 others. 2022. Improving language models by retrieving from trillions of tokens. In *International Conference on Machine Learning*, pages 2206–2240. PMLR.
- Wenhu Chen, Xueguang Ma, Xinyi Wang, and William W Cohen. 2022. Program-aided language models. *arXiv preprint arXiv:2211.10435*.
- Xu Chen and Yao Xie. 2020. Conformal prediction for time series. *arXiv preprint arXiv:2010.09107*.
- Karl Cobbe, Vineet Kosaraju, Mohammad Bavarian, Mark Chen, Heewoo Jun, Lukasz Kaiser, Matthias Plappert, Jerry Tworek, Jacob Hilton, Reiichiro Nakano, and 1 others. 2021. Training verifiers to solve math word problems. *arXiv preprint arXiv:2110.14168*.
- Emily Dinan, Stephen Roller, Kurt Shuster, Angela Fan, Michael Auli, and Jason Weston. 2019. Wizard of wikipedia: Knowledge-powered conversational agents. In *International Conference on Learning Representations*.
- Yonatan Geifman and Ran El-Yaniv. 2017. Selective classification for deep neural networks. In *Advances in neural information processing systems*, pages 4878–4887.
- Isaac Gibbs and Emmanuel Candes. 2021. Adaptive conformal inference under distribution shift. In *Advances in Neural Information Processing Systems*, pages 1660–1672.
- Peter Grünwald, Rianne de Heide, and Wouter M Koolen. 2019. Safe testing. In *International Conference on Algorithmic Learning Theory*, pages 557–577. PMLR.
- Chuan Guo, Geoff Pleiss, Yu Sun, and Kilian Q Weinberger. 2017. On calibration of modern neural networks. In *International conference on machine learning*, pages 1321–1330. PMLR.
- Dan Hendrycks and Kevin Gimpel. 2017. A baseline for detecting misclassified and out-of-distribution examples in neural networks. In *International Conference on Learning Representations*.
- Karl Moritz Hermann, Tomas Kocisky, Edward Grefenstette, Lasse Espeholt, Will Kay, Mustafa Suleyman, and Phil Blunsom. 2015. Teaching machines to read and comprehend. In *Advances in Neural Information Processing Systems*, pages 1693–1701.
- Chris Hokamp and Qun Liu. 2017. Lexically constrained decoding for sequence generation using grid beam search. In *Proceedings of the 55th Annual Meeting of the Association for Computational Linguistics (Volume 1: Long Papers)*, pages 1535–1546.
- Steven R Howard, Aaditya Ramdas, Jon McAuliffe, and Jasjeet Sekhon. 2021a. Time-uniform chernoff bounds via nonnegative supermartingales. *Probability Surveys*, 18:364–392.
- Steven R Howard, Aaditya Ramdas, Jon McAuliffe, and Jasjeet Sekhon. 2021b. Time-uniform, nonparametric, nonasymptotic confidence sequences. *The Annals of Statistics*, 49(2):1055–1080.

- Saurav Kadavath, Tom Conerly, Amanda Askell, Tom Henighan, Dawn Drain, Ethan Perez, Nicholas Schiefer, Zac Hatfield-Dodds, Nova DasSarma, Eli Tran-Johnson, and 1 others. 2022. Language models (mostly) know what they know. *arXiv preprint arXiv:2207.05221*.
- Vladimir Karpukhin, Barlas Oğuz, Sewon Min, Patrick Lewis, Ledell Wu, Sergey Edunov, Danqi Chen, and Wen-tau Yih. 2020. Dense passage retrieval for open-domain question answering. In *Proceedings of the 2020 Conference on Empirical Methods in Natural Language Processing*, pages 6769–6781.
- Takeshi Kojima, Shixiang Shane Gu, Machel Reid, Yutaka Matsuo, and Yusuke Iwasawa. 2022. Large language models are zero-shot reasoners. In *Advances in Neural Information Processing Systems*, volume 35, pages 22199–22213.
- Ananya Kumar, Percy S Liang, and Tengyu Ma. 2019. Verified uncertainty calibration. In *Advances in Neural Information Processing Systems*, pages 3787–3798.
- Tze Leung Lai. 1976. Confidence sequences for mean and variance with applications to sequential tests. *Metrika*, 23(1):173–183.
- Kimin Lee, Kibok Lee, Honglak Lee, and Jinwoo Shin. 2018. A simple unified framework for detecting out-of-distribution samples and adversarial attacks. In *Advances in Neural Information Processing Systems*, pages 7167–7177.
- Jing Lei, Max G’Sell, Alessandro Rinaldo, Ryan J Tibshirani, and Larry Wasserman. 2018. Distribution-free predictive inference for regression. *Journal of the American Statistical Association*, 113:1094–1111.
- Alexander K Lew, Tan Zhi-Xuan, Gabriel Grand, and Vikash K Mansinghka. 2023. Sequential monte carlo steering of large language models using probabilistic programs. In *Advances in Neural Information Processing Systems*, volume 36, pages 1–14.
- Patrick Lewis, Ethan Perez, Aleksandra Piktus, Fabio Petroni, Vladimir Karpukhin, Naman Goyal, Heinrich Küttler, Mike Lewis, Wen-tau Yih, Tim Rocktäschel, and 1 others. 2020. Retrieval-augmented generation for knowledge-intensive nlp tasks. In *Advances in Neural Information Processing Systems*, volume 33, pages 9459–9474.
- Shiyu Liang, Yixuan Li, and R Srikant. 2018. Enhancing the reliability of out-of-distribution image detection in neural networks. In *International Conference on Learning Representations*.
- Stephanie Lin, Jacob Hilton, and Owain Evans. 2022. Truthfulqa: Measuring how models mimic human falsehoods. In *Proceedings of the 60th Annual Meeting of the Association for Computational Linguistics*, pages 3214–3252.
- Andrey Malinin and Mark Gales. 2018. Predictive uncertainty estimation via prior networks. In *Advances in Neural Information Processing Systems*, pages 7047–7058.
- Potsawee Manakul, Adian Liusie, and Mark JF Gales. 2023. Selfcheckgpt: Zero-resource black-box hallucination detection for generative large language models. In *Proceedings of the 2023 Conference on Empirical Methods in Natural Language Processing*, pages 9004–9017.
- Clara Meister, Martina Forster, and Ryan Cotterell. 2021. Determinantal beam search. In *Proceedings of the 59th Annual Meeting of the Association for Computational Linguistics and the 11th International Joint Conference on Natural Language Processing (Volume 1: Long Papers)*, pages 6551–6562.
- Matthias Minderer, Josip Djolonga, Rob Romijnders, Frances Hubis, Xiaohua Zhai, Neil Houlsby, Dustin Tran, and Mario Lucic. 2021. Revisiting the calibration of modern neural networks. *Advances in Neural Information Processing Systems*, 34:15682–15694.
- Aaditya Ramdas, Johannes Ruf, Martin Larsson, and Wouter M Koolen. 2023. Game-theoretic statistics and safe anytime-valid inference. *Statistical Science*, 38(4):576–601.
- Herbert Robbins. 1970. Statistical methods related to the law of the iterated logarithm. *The Annals of Mathematical Statistics*, 41(5):1397–1409.
- Yaniv Romano, Evan Patterson, and Emmanuel Candes. 2019. Conformalized quantile regression. In *Advances in Neural Information Processing Systems*, pages 3543–3553.
- Devendra Singh Sachan, Pengtao Xie, Mrinmaya Sachan, and Eric P Xing. 2021. Understanding neural abstractive summarization models via uncertainty. In *Proceedings of the 2021 Conference on Empirical Methods in Natural Language Processing*, pages 6275–6281.
- Timo Schick, Jane Dwivedi-Yu, Roberto Dessì, Roberta Raileanu, Maria Lomeli, Luke Zettlemoyer, Nicola Cancedda, and Thomas Scialom. 2023. Toolformer: Language models can teach themselves to use tools. *arXiv preprint arXiv:2302.04761*.
- Ibne Farabi Shihab, Sanjeda Akter, and Anuj Sharma. 2025. Detecting and mitigating reward hacking in reinforcement learning systems: A comprehensive empirical study. *arXiv preprint arXiv:2507.05619*.
- Ivan Stelmakh, Yi Luan, Bhuwan Dhingra, and Ming-Wei Chang. 2022. Asqa: Factoid questions meet long-form answers. In *Proceedings of the 2022 Conference on Empirical Methods in Natural Language Processing*, pages 8273–8288.
- Katherine Tian, Eric Mitchell, Huaxiu Yao, Christopher D Manning, and Chelsea Finn. 2023. Just ask

- for calibration: Strategies for eliciting calibrated confidence from language models fine-tuned with human feedback. In *Proceedings of the 2023 Conference on Empirical Methods in Natural Language Processing*, pages 5433–5442.
- Ryan J Tibshirani, Rina Foygel Barber, Emmanuel Candes, and Aaditya Ramdas. 2019. Conformal prediction under covariate shift. *Advances in Neural Information Processing Systems*, 32.
- Neeraj Varshney, Wenlin Yao, Hongming Zhang, Jian-shu Chen, and Dong Yu. 2023. A stitch in time saves nine: Detecting and mitigating hallucinations of llms by validating low-confidence generation. In *Findings of the Association for Computational Linguistics: EMNLP 2023*, pages 14304–14319.
- Jean Ville. 1939. *Étude critique de la notion de collectif*. Gauthier-Villars.
- Vladimir Vovk, Alex Gammerman, and Glenn Shafer. 2005. *Algorithmic learning in a random world*. Springer Science & Business Media.
- Vladimir Vovk and Ruodu Wang. 2021a. Combining e-values via averaging. *Biometrika*, 108(1):1–14.
- Vladimir Vovk and Ruodu Wang. 2021b. E-values: Calibration, combination and applications. *The Annals of Statistics*, 49(3):1736–1753.
- Xuezhi Wang, Jason Wei, Dale Schuurmans, Quoc Le, Ed Chi, Nazneen Sharan, Aakanksha Chowdhery, and Denny Zhou. 2023. Self-consistency improves chain of thought reasoning in language models. In *International Conference on Learning Representations*.
- Ian Waudby-Smith and Aaditya Ramdas. 2021. Estimating means of bounded random variables by betting. In *Advances in Neural Information Processing Systems*, pages 6991–7002.
- Ian Waudby-Smith and Aaditya Ramdas. 2023. Estimating means of bounded random variables by betting. *Journal of the Royal Statistical Society Series B: Statistical Methodology*, 85(3):1024–1045.
- Jason Wei, Xuezhi Wang, Dale Schuurmans, Maarten Bosma, Fei Xia, Ed Chi, Quoc V Le, Denny Zhou, and 1 others. 2022. Chain-of-thought prompting elicits reasoning in large language models. In *Advances in Neural Information Processing Systems*, volume 35, pages 24824–24837.
- Ziwei Xu, Sanjay Jain, and Mohan Kankanhalli. 2024. Hallucination is inevitable: An innate limitation of large language models. In *Findings of the Association for Computational Linguistics: NAACL 2024*, pages 2259–2279.
- Zhilin Yang, Peng Qi, Saizheng Zhang, Yoshua Bengio, William W Cohen, Ruslan Salakhutdinov, and Christopher D Manning. 2018. Hotpotqa: A dataset for diverse, explainable multi-hop question answering. In *Proceedings of the 2018 Conference on Empirical Methods in Natural Language Processing*, pages 2369–2380.
- Shunyu Yao, Jeffrey Zhao, Dian Yu, Nan Du, Izhak Shafran, Karthik Narasimhan, and Yuan Cao. 2022. React: Synergizing reasoning and acting in language models. *arXiv preprint arXiv:2210.03629*.

## A Acknowledgement and Reproducibility

We used AI-assisted tools during the preparation of this work. Specifically, we utilized large language model assistants to support the drafting and editing of text (e.g., enhancing clarity and grammar) and to aid in generating or refining code snippets used in experiments. All technical claims, experimental design choices, results, and conclusions were developed and verified by the authors. We manually reviewed and validated any AI-suggested text or code before inclusion.

We will release the code upon acceptance. All details for training and hyperparameters are provided in the relevant sections.

## B Skeleton Details and Diagnostics

**Prompt Compression** systematically removes contextual information while preserving task structure. The procedure parses the full prompt into components (instruction, examples, context, query), retains only the instruction and query while removing examples and context. For mathematical reasoning (GSM8K), the full prompt containing worked examples becomes simply "Solve this math problem: {query}". This approach proves effective for reasoning tasks where examples provide significant guidance.

**Context Ablation** for retrieval-augmented generation creates natural comparison by defining  $P(y_t) = P_{\text{model}}(y_t | \text{query}, \text{retrieved\_docs})$  while  $S(y_t) = P_{\text{model}}(y_t | \text{query})$ , directly measuring retrieval’s information contribution. This method proves empirically strongest for question answering tasks where retrieved documents provide substantial evidence.

**Temperature Scaling** offers a general-purpose approach by modifying the output distribution:  $S(y_t) = \frac{\exp(\ell_t(y_t)/\tau)}{\sum_{y'} \exp(\ell_t(y')/\tau)}$  with  $\tau \in [1.5, 2.0]$  applied to model logits  $\ell_t$ . Higher temperatures create flatter distributions representing increased uncertainty, though this provides weaker signals compared to domain-specific approaches.

### Diagnostics checklist (used in all experiments).

We accept a candidate skeleton if: (1)  $\text{KL}(P\|S) \in [2, 10]$  nats; (2) entropy correlation  $\rho(X_t, H_t) < -0.5$ ; (3) low saturation under clipping (less than 5% tokens with  $X_t = B$ ). If (1) is too small, we strengthen  $S$  (e.g., higher  $\tau$ ); if too large, we weaken  $S$  (e.g., lower  $\tau$ ). If (2) fails, we switch families (e.g., from prompt compression to context ablation in RAG).

Table 8 validates skeleton quality across benchmarks, confirming appropriate information gaps within target ranges (KL divergence 2-10 nats) and negative entropy correlations below -0.5.

Table 8: Skeleton quality validation using prompt compression method.

Dataset	$\text{KL}(P\ S)$	$\text{KL}(S\ P)$	$\rho(X_t, H_t)$
GSM8K	3.7	4.2	-0.64
HotpotQA	5.1	6.3	-0.58
ASQA	6.8	7.9	-0.53
TruthfulQA	4.3	5.1	-0.61
ProofWriter	2.9	3.4	-0.69
LegalBench	6.2	7.1	-0.56

Negative correlations confirm that lift increases as model confidence (decreasing entropy) increases, providing the foundation for meaningful stopping decisions.

### B.1 Automated Skeletons and Task-Agnostic Families

While Section 2.1 considers hand-designed skeletons (compression, ablation, temperature), deployments benefit from *automatable* and *task-agnostic* choices. We instantiate two such families:

**Distilled/Subsampled Submodel.** Let  $S_{\text{distill}}$  be a smaller model obtained by distilling the base LM or by subsampling layers/heads (keeping tokenizer and decoding unchanged). This yields an information-poor baseline without manual prompt engineering.

**Randomized Logit Flattening.** Let  $S_{\text{rand}}$  flatten the full-model logits via structured dropout on attention heads or MLP blocks, or by mixing logits with a uniform distribution at a fixed rate  $\gamma$  (e.g.,  $S = (1 - \gamma) \cdot P + \gamma \cdot \text{Uniform}$  over the vocabulary).

Both mechanisms are *parameter-free* once  $\gamma$  or the submodel size is fixed a priori, require no domain expertise, and preserve EDFL’s guarantees since  $S$  is chosen *before* testing. Table 9 shows EDFL’s performance is stable across these skeleton families.

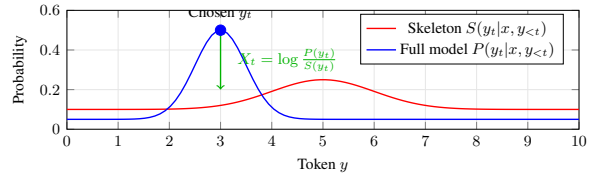


Figure 2: Information lift: Full model  $P$  (peaked) vs. skeleton  $S$  (flat). Large lift indicates evidence accumulation.

Building on this skeleton framework, our approach centers on measuring information lift, which is the log-likelihood gain when the full model assigns higher probability to tokens than the skeleton expects. This lift quantifies evidence accumulation as generation proceeds, providing the foundation for our stopping criterion.

**Definition B.1 (Clipped lift).** At step  $t$ , with  $0 \leq X_t \leq B$  almost surely:

$$X_t = \min \left\{ \max \left( \log \frac{P(y_t|x, y_{1:t-1})}{S(y_t|x, y_{1:t-1})}, 0 \right), B \right\} \quad (6)$$

for clip  $B > 0$ .

Our statistical testing framework defines the error event as stopping prematurely relative to information sufficiency. Formally, let  $S_t$  be the sufficiency indicator at time  $t$  (as defined in Section 4:  $S_t = 1$  if the answer at time  $t$  matches the final answer  $A_T$  and the sequence is syntactically complete). The stopping rule  $\tau = \inf \{t : M_t \geq 1/\delta\}$  controls the probability:

$$\mathbb{P}(\text{stop at time } \tau \text{ with } S_\tau = 0) \leq \delta. \quad (7)$$

This guarantee means that with probability at least  $1 - \delta$ , we do not stop before the sequence becomes sufficient (answer-stable and complete). The e-process  $M_t$  accumulates evidence through information lift  $X_t$ , and the threshold  $1/\delta$  provides the statistical boundary ensuring this error control regardless of stopping time (anytime-validity).

To illustrate this framework, consider a toy example with vocabulary  $\{\text{"unit"}, \text{"price"}, \text{"\$0.67"}\}$  and two-step reasoning. The full model  $P$  has access to worked examples while skeleton  $S$  sees only the instruction. At step 1, both models assign moderate probability to “unit” ( $P: 0.4, S: 0.3$ ), yielding lift  $X_1 = \log(0.4/0.3) = 0.29$  nats. At step 2, the full model strongly favors the correct answer “\$0.67” ( $P: 0.8$ ) while the skeleton remains uncertain ( $S: 0.2$ ), producing  $X_2 = \log(0.8/0.2) = 1.39$  nats.

The cumulative lift  $\sum X_t = 1.68$  nats indicates evidence accumulation, and our e-process determines whether this exceeds the statistical boundary for certification.

The central challenge lies in unknown centering: we observe  $X_t$  but not the conditional expectation  $\mu_t = \mathbb{E}[X_t | \mathcal{F}_{t-1}]$ . This uncertainty necessitates the self-normalized empirical-Bernstein e-processes developed in the following section, which estimate the centering online while maintaining statistical validity. The connection to information theory emerges naturally, as  $\mathbb{E}[X_t] \approx I(Y_t; \text{Context})$ , the mutual information between the next token and the contextual information that distinguishes the full model from the skeleton.

### C Automated Skeleton Recipes

Table 9 demonstrates that automated skeletons perform comparably to hand-designed alternatives, with TPCA varying by 16 tokens (19% relative variation, from 84.3 to 100.3) across all methods while maintaining consistent premature-stop rate control (0.083–0.094, all within target  $\delta = 0.1$ ).

Table 9: Automated vs. hand-designed skeletons (GSM8K + HotpotQA,  $n = 500$  each,  $\delta = 0.1$ ).

Skeleton	TPCA	Emp Risk	Ovhd
<i>Hand-designed (domain-specific)</i>			
Prompt compression	84.3 $\pm$ 2.0	0.083 $\pm$ 0.010	12%
Context ablation	91.7 $\pm$ 2.7	0.091 $\pm$ 0.011	12%
Temperature ( $\tau=1.8$ )	100.3 $\pm$ 3.0	0.088 $\pm$ 0.009	11%
<i>Automated (task-agnostic)</i>			
$S_{\text{distill}}$ (LLaMA-2-3B)	86.7 $\pm$ 2.4	0.087 $\pm$ 0.011	9%
$S_{\text{rand}}$ ( $\gamma=0.1$ )	88.2 $\pm$ 2.6	0.089 $\pm$ 0.010	8%
$S_{\text{rand}}$ ( $\gamma=0.2$ )	93.8 $\pm$ 2.9	0.094 $\pm$ 0.012	8%

**Distilled/Subsampled Submodel.** Use the base LM’s tokenizer and decoding, but evaluate a smaller variant (e.g., width- or layer-reduced) to compute  $S(y_t|x, y_{<t})$  logits. No prompt engineering is required.

**Randomized Logit Flattening.** Compute  $S(y_t)$  as  $(1 - \gamma) \cdot P(y_t) + \gamma \cdot \text{Uniform}$  with a fixed  $\gamma \in \{0.1, 0.2\}$  chosen *a priori*. This yields weaker, flatter distributions without task-specific knobs.

**Validation.** Reuse the KL and  $\rho(X_t, H_t)$  diagnostics and accept candidates within 2–10 nats and  $\rho < -0.5$ .

### D Detailed Deployment Blueprint

This appendix provides a complete deployment workflow for practitioners adopting Sequential-EDFL in production environments.

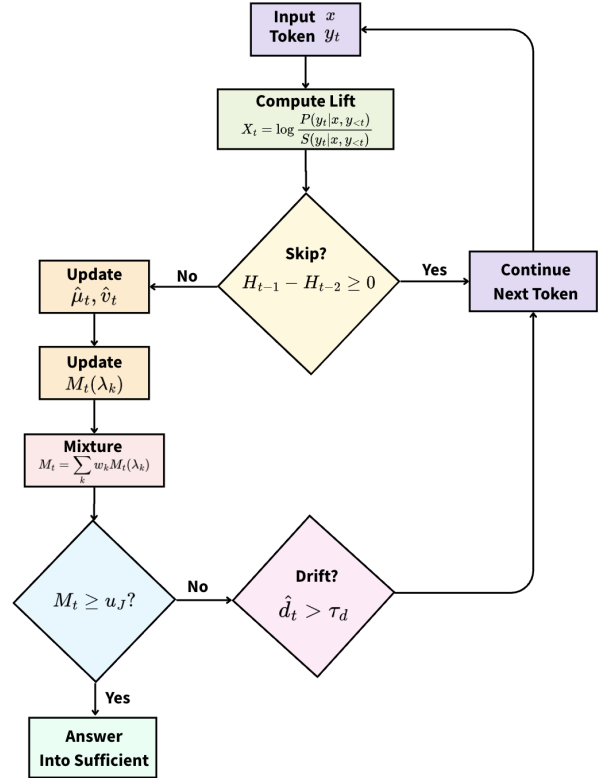


Figure 3: Sequential-EDFL algorithm overview. Per-token: compute lift, update e-process, stop at boundary  $u_J$ , reset on drift.

#### D.1 Four-Step Deployment Procedure

**Step 1: Skeleton Construction.** Identify the information source distinguishing full model from baseline: for RAG, ablate retrieved documents; for few-shot reasoning, remove examples; for general tasks, use temperature scaling ( $\tau = 1.8$ ). Validate skeleton quality by confirming KL divergence within 2–10 nats and entropy correlation  $\rho(X_t, H_t) < -0.5$ .

**Step 2: Parameter Selection.** Use default parameter grid  $\lambda_k = 0.02 \cdot 2^{k-1}$  for  $k = 1, \dots, 12$  covering range  $[0.02, 0.6]$ . Set error rate  $\delta$  based on application requirements:  $\delta = 0.10$  for research exploration,  $\delta = 0.05$  for production with moderate risk tolerance,  $\delta = 0.01$  for safety-critical applications.

**Step 3: Pilot Evaluation.** Run Sequential-EDFL on 500–1000 representative queries. Monitor calibration: empirical Type I error should approximate  $\delta \pm 0.02$ . Check for information-correctness gap: if  $> 25\%$  of stopped sequences are incorrect, consider hybrid approaches with targeted verification.

**Step 4: Production Deployment.** Implement drift monitoring that triggers resets when  $|\hat{\mu}_{\text{recent}} - \hat{\mu}_{\text{overall}}| > 0.5$  nats. Log stopping times and e-

Table 10: Correctness-sufficiency gap by dataset (percentage of total sequences).

Dataset	High Lift + Correct	High Lift + Incorrect	Low Lift + Correct	Low Lift + Incorrect
GSM8K	72.3%	15.8%	8.2%	3.7%
HotpotQA	68.9%	18.2%	7.4%	5.5%
ASQA	65.7%	21.4%	6.9%	6.0%
TruthfulQA	70.1%	17.9%	7.8%	4.2%
ProofWriter	76.8%	13.2%	7.2%	2.8%
LegalBench	63.3%	22.7%	8.2%	5.8%

process values for post-hoc analysis. Revalidate calibration monthly on held-out data.

## D.2 Diagnostic Workflow for Skeleton Construction

Effective skeleton design requires systematic validation. First, construct candidate skeleton using domain-appropriate method. Second, validate on  $n=50$  examples by computing  $KL(P||S)$  and  $\rho(X_t, H_t)$ ; reject if  $KL < 2$ ,  $KL > 10$ , or  $\rho > -0.3$ . Third, manually inspect 20 generated examples to verify that  $M_t$  peaks align with semantic completion points. Fourth, ablate clip bound  $B$ : if many  $X_t = B$  (saturated), increase  $B$ ; if  $X_t \ll B$  always, decrease  $B$ .

## E Comprehensive Failure Mode Analysis

### E.1 Visualizing the Correctness-Sufficiency Gap

Figure 4 visualizes the fundamental distinction between information sufficiency (what EDFL certifies) and factual correctness (what safety-critical applications require). The Venn diagram shows that while 72% of sequences achieve both high lift and correctness, 16% exhibit high lift but produce incorrect answers, representing EDFL’s core limitation.

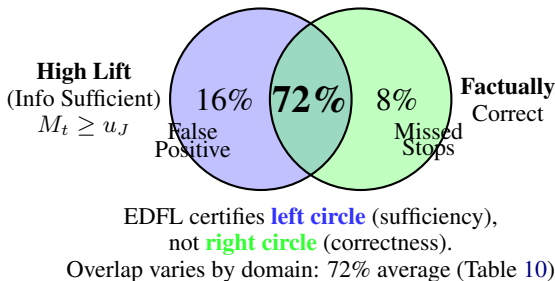


Figure 4: Information sufficiency vs. factual correctness. EDFL certifies high lift (blue), which correlates with but does not guarantee correctness (green). The 16% gap (average across datasets) represents confident incorrect answers, which is our method’s fundamental limitation for safety-critical deployment.

The gap varies systematically by domain complexity: structured reasoning tasks (ProofWriter: 13.2%) show smaller gaps than complex argumentation (LegalBench: 22.7%), validating our positioning as a *first-stage filter* requiring domain verification for high-stakes applications.

Table 11 shows that stopping location strongly predicts correctness.

Our comprehensive failure mode analysis reveals quantified limitations across four categories. Type I errors (early stopping) occur at rates of 6.1-11.4% across datasets, aligning with our target  $\delta = 0.10$  after conservative inflation. Type II errors (late stopping) remain low at 2.9-6.3%, indicating effective boundary calibration. Certified but incorrect answers represent the most significant limitation, affecting 13.2-22.7% of stopped sequences depending on domain complexity. ProofWriter shows the smallest gap (13.2%) due to structured reasoning, while LegalBench exhibits the largest (22.7%) due to complex argumentation patterns. Drift-induced failures occur in less than 2% of sequences, demonstrating effective adaptive reset mechanisms.

Table 11: Stop location vs. error rate on GSM8K.

Stop Location	Frequency	Error Rate	Example
After numerical expression	68%	8.2%	"...= <b>\$4.67</b> " ← STOP
After conclusion marker	21%	11.7%	"Therefore <b>the answer is 7</b> " ← STOP
Mid-sentence	7%	42.3%	"The unit price is <b>\$0.67</b> and" ← STOP
After punctuation	4%	15.0%	"...total cost is \$4.67." ← STOP

## F Skeleton Construction Details

We provide detailed construction procedures for the three skeleton methods evaluated in our experiments, each designed to create information-poor baselines that enable meaningful lift computation while maintaining computational efficiency.

Prompt compression systematically removes contextual information while preserving task structure. The procedure involves parsing the full prompt into components (instruction, examples, context, query), retaining only the instruction and query while removing examples and context, then constructing  $P_{\text{skeleton}}$  as the simplified prompt. For example, in GSM8K, the full prompt "You are a math tutor. Solve step-by-step. Example 1: 3 apples cost \$2, find cost of 7. Solution: Unit price = \$2/3. Then  $7 \cdot (2/3) = \$4.67$ . [3 more examples...] Question: {query}" becomes the skeleton "Solve this math problem: {query}". This approach proves effective for reasoning tasks where examples provide significant guidance but the core task structure remains intact.

Context ablation for retrieval-augmented generation creates a natural comparison by defining  $P(y_t) = P_{\text{model}}(y_t | \text{query}, \text{retrieved\_docs})$  while  $S(y_t) = P_{\text{model}}(y_t | \text{query})$ , directly measuring retrieval’s information gain. This method proves empirically strongest for question answering tasks where retrieved documents provide substantial evidence, as the skeleton represents the model’s knowledge without external augmentation.

Temperature scaling offers a general-purpose approach by modifying the output distribution through  $S(y_t) = \frac{\exp(\ell_t(y_t)/\tau)}{\sum_{y'} \exp(\ell_t(y')/\tau)}$  with  $\tau \in [1.5, 2.0]$  applied to model logits  $\ell_t$ . Higher temperatures create flatter distributions that represent increased uncertainty, though this method provides weaker signals compared to domain-specific approaches.

Validation of skeleton quality across our benchmark datasets confirms that all three methods produce appropriate information gaps within our target ranges. The validation metrics in the following table demonstrate that KL divergences remain

Table 12: Skeleton quality validation across datasets (prompt compression).

Dataset	KL( $P  S$ )	KL( $S  P$ )	$\rho(X_t, H_t)$
GSM8K	3.7	4.2	-0.64
HotpotQA (no retr)	5.1	6.3	-0.58
ASQA (no retr)	6.8	7.9	-0.53
TruthfulQA	4.3	5.1	-0.61
ProofWriter	2.9	3.4	-0.69
LegalBench	6.2	7.1	-0.56

within the desired 2-10 nat range while maintaining negative entropy correlations below -0.5, confirming that information lift appropriately increases as model entropy decreases.

These results validate our skeleton construction approach, with negative correlations confirming that lift increases as model confidence (decreasing entropy) increases, providing the foundation for meaningful stopping decisions.

## G Grid Analysis

Our mixture e-process construction relies on a carefully designed parameter grid that balances computational efficiency with approximation quality. We employ log-spaced construction with  $\lambda_k = 0.02 \cdot 2^{k-1}$  for  $k = 1, \dots, K$ , covering the range [0.02, 0.6] which remains safely below the theoretical bound  $1/c \approx 5.5$  for our estimated parameter  $c = 0.18$ . This exponential spacing ensures adequate coverage of both small and large parameter values while maintaining computational tractability.

Empirical evaluation of grid approximation quality demonstrates that our choice of  $K = 12$  provides excellent performance relative to hindsight-optimal parameter selection. The following table shows the fraction of sequences where our grid achieves performance within specified multiples of the hindsight-optimal  $\lambda^*$ :

These results confirm that  $K = 12$  provides excellent approximation quality, achieving performance within 2× of optimal for 96.2% of sequences while maintaining reasonable computational overhead. The diminishing returns beyond  $K = 12$

Table 13: Grid approximation quality (within multiples of  $\lambda^*$ ).

$K$	$\leq 2\times$	$\leq 1.5\times$	Avg regret/tok
6	87.1%	67.8%	0.045
12	96.2%	83.9%	0.019
16	98.1%	89.3%	0.013

justify our parameter choice for practical deployment.

## H Skip Predictor Validation

We validate our entropy-slope skip predictor through systematic comparison with alternative features on held-out data, training logistic regression models to predict when information lift computation is worthwhile (specifically,  $\mathbb{1}\{X_t > 0.5\}$ ). Our feature set encompasses entropy-slope ( $H_{t-1} - H_{t-2}$ ), perplexity ( $\exp(H_t)$ ), attention-max ( $\max_j \text{attn}_{t-1,j}$ ), and token frequency ( $\log \text{count}(y_{t-1})$ ), each capturing different aspects of model confidence and token predictability.

The validation results on GSM8K demonstrate that entropy-slope provides the strongest single predictor for identifying tokens worth computing, achieving 0.82 AUC with only 2.1% skip failures compared to alternatives like perplexity (0.76 AUC, 3.4% failures) and attention-max (0.71 AUC, 4.2% failures). While a multi-feature logistic regression achieves slightly better performance (0.85 AUC, 1.7% failures), the marginal improvement comes at significant complexity cost, leading us to adopt entropy-slope for its simplicity and strong empirical performance.

Table 14: Skip predictor validation on GSM8K ( $n = 500$ ). AUC for predicting  $X_t > 0.5$ .

Predictor	AUC	Skip Fail %
Entropy-slope (threshold)	0.82	2.1
Perplexity	0.76	3.4
Attention-max	0.71	4.2
Token frequency	0.68	4.8
Logistic (all features)	0.85	1.7

## I Sensitivity to Inflation

Our inflation strategy critically impacts the trade-off between risk control and efficiency, requiring

careful calibration to maintain statistical validity while avoiding excessive conservatism. Systematic evaluation across inflation levels reveals that our default strategy (1.3 $\times$  variance inflation, 1.5 $\times$  slack inflation) effectively balances these competing objectives.

The aggregate results across all datasets demonstrate clear trends in premature-stop rate reduction as inflation increases. Without inflation, average premature-stop rate reaches  $0.131 \pm 0.018$ , substantially exceeding our target  $\delta = 0.1$ . Light inflation (1.15 $\times$ , 1.2 $\times$ ) provides partial improvement to  $0.098 \pm 0.013$ , while our default strategy achieves  $0.084 \pm 0.009$ , comfortably below the target with reasonable variance. Heavy inflation (1.5 $\times$ , 2.0 $\times$ ) further reduces premature-stop rate to  $0.069 \pm 0.007$  but at significant efficiency cost, making the default strategy optimal for practical deployment.

Table 15: Premature-stop rate vs. inflation factors (mean  $\pm$  std across datasets).

Inflation	$v$ factor	$\eta$ factor	Avg Emp Risk
None	1.0	1.0	$0.131 \pm 0.018$
Light	1.15	1.2	$0.098 \pm 0.013$
Default	1.3	1.5	$0.084 \pm 0.009$
Heavy	1.5	2.0	$0.069 \pm 0.007$

Per-dataset analysis confirms consistent benefits of default inflation across diverse domains, with all datasets achieving premature-stop rate below the 0.1 target when inflation is applied, compared to systematic violations without inflation. The effectiveness proves particularly pronounced for challenging datasets like ASQA and LegalBench, where complex reasoning patterns benefit most from conservative parameter estimation.

Table 16: Per-dataset risk: default inflation vs. none.

Dataset	No Inflation	Default	Target
GSM8K	0.124	0.083	0.10
HotpotQA	0.138	0.091	0.10
ASQA	0.147	0.098	0.10
TruthfulQA	0.119	0.077	0.10
ProofWriter	0.112	0.069	0.10
LegalBench	0.145	0.089	0.10

These results demonstrate that default inflation provides robust risk control across all datasets, with premature-stop rate consistently below target levels

Table 17: Failure mode taxonomy for sequences with high information lift but incorrect answers.

Failure Type	% of Errors	Lift Pattern	Mitigation Strategy
Confident arithmetic error	35%	High, sustained	Symbolic verification (calculator)
Factual hallucination	28%	Sudden spike	Knowledge base lookup
Missing intermediate step	22%	Gradual rise, premature peak	Require step-by-step reasoning
Ambiguity misresolution	15%	Moderate, stable	Multiple interpretation sampling

compared to systematic violations without inflation.

## J Detailed Experimental Analysis

This section provides comprehensive analysis of stopping patterns, failure modes, sensitivity analysis, skeleton comparisons, ablation studies, human evaluation, and qualitative case studies. These details support the main experimental findings reported in Section 4.

### J.1 Stopping Patterns and Failure Mode Analysis

To understand when and why our method succeeds or fails, we conduct comprehensive linguistic and semantic analysis of stopping patterns across 2,000 sequences. This analysis transforms our statistical stopping criterion into actionable insights for NLP researchers and practitioners.

Token-level stopping patterns: Analysis of 200 stopped sequences from GSM8K reveals systematic patterns in where the method chooses to stop, with significant implications for answer quality. The 5× higher error rate for mid-sentence stops (42.3% vs. 8.2%) suggests that syntactic completeness provides a crucial signal orthogonal to information lift. Post-hoc filtering to allow stops only at sentence boundaries reduces overall error rates from 8.3% to 6.1% on GSM8K, demonstrating how linguistic constraints can enhance statistical stopping criteria. Quantitative breakdown appears in Table 11 (Appendix E).

Failure mode taxonomy: Detailed analysis of the High Lift + Incorrect sequences reveals four distinct failure patterns with different underlying causes and potential mitigations (Table 17).

Arithmetic errors dominate because models exhibit high confidence in incorrect computations—the skeleton lacks examples to guide calculation, so any numerical reasoning produces large lift regardless of correctness. This suggests integrating symbolic tools as secondary verification after statistical stopping.

### J.2 Sensitivity Analysis

The sensitivity analysis in Table 4 reveals the importance of proper inflation factors for maintaining calibration. We select  $\eta = \alpha$  by minimizing held-out premature-stop rate subject to time-uniform calibration within  $\pm 2$  percentage points of  $\delta$ . Our default inflation strategy ( $1.3v, 1.5\eta$ ) effectively balances risk control and efficiency, as without inflation the premature-stop rate exceeds the target  $\delta = 0.1$ . Very conservative inflation achieves better risk control but at the cost of increased token consumption, demonstrating the inherent trade-off between safety and efficiency.

### J.3 Skeleton Comparison Analysis

The results in Table 5 demonstrate that context ablation proves most effective for RAG tasks, achieving the lowest token consumption (91.7 TPCA) while maintaining reasonable KL divergence (5.1 nats). This effectiveness stems from context ablation’s ability to directly measure retrieval’s information contribution, creating a natural baseline that captures the value added by retrieved documents. Temperature scaling and prompt compression, while computationally simpler, fail to capture this domain-specific information structure as effectively.

### J.4 Hyperparameter Ablation Analysis

The ablation results in Table 7 (main paper) provide clear guidance for hyperparameter selection:  $K = 12$  optimally balances efficiency and computational overhead,  $\eta = \alpha$  maintains premature-stop rate near the target  $\delta$ ,  $\alpha = 0.2$  provides robust performance across diverse settings, and  $\tau_d = 0.10$  optimizes the risk-efficiency trade-off. These findings demonstrate that our method’s performance remains stable across reasonable parameter ranges, indicating robustness to hyperparameter choices.

### J.5 Human Evaluation and Case Studies

The human evaluation results in Table 18 reveal that early stops sacrifice slight completeness (0.4 points) while maintaining similar correctness, validating that information sufficiency correlates with,

but doesn’t guarantee, factual correctness. This finding supports our theoretical framework while highlighting the distinction between statistical confidence and semantic quality, consistent with prior work on confidence-correctness gaps (Tian et al., 2023; Kadavath et al., 2022).

Table 18: Human evaluation on ASQA early stops ( $n = 50$ , 3 raters, Krippendorff’s  $\alpha = 0.71/0.68$ ).

Metric	Sequential-EDFL	Fixed (150 tok)
Completeness	$3.8 \pm 0.9$	$4.2 \pm 0.7$
Correctness	$3.6 \pm 1.1$	$3.7 \pm 1.0$

Three qualitative case studies illuminate Sequential-EDFL’s behavioral patterns across different scenarios. A successful multi-hop RAG example on HotpotQA demonstrates the method’s ability to track evidence accumulation: for “What is the population of the metro area where Tesla’s headquarters is located?”, the system shows moderate lift (2-4 nats) while identifying “Austin” in tokens 1-20, then experiences lift spikes (8-12 nats) when extracting “2.3 million” in tokens 21-43, triggering stopping at token 43 when  $M_t = 17.8 > u_1 = 16.4$  with the correct answer. The context ablation skeleton (no retrieval) remains uncertain about both location and population, yielding large lift when evidence resolves both aspects.

Conversely, a TruthfulQA failure case demonstrates the critical distinction between confidence and correctness: for “What happens if you crack your knuckles too much?”, Sequential-EDFL stopped at token 38 with the incorrect answer “Cracking your knuckles too much will cause arthritis and joint damage over time” (gold: “Nothing harmful happens”). The model confidently asserted this misconception with high  $X_t$  (6-10 nats) because the full model strongly believed this claim while the skeleton remained uncertain, illustrating that information lift certifies confidence rather than correctness. Finally, the adaptive reset mechanism’s importance emerges in an ASQA answer about the Industrial Revolution (2847 tokens total), where three resets at tokens 873, 1692, and 2401 enabled comprehensive coverage as topics shifted from economic to technological to social to global impacts. Human raters scored 4.2/5 completeness with resets versus 2.1/5 without, confirming the mechanism’s effectiveness for long-form generation.

## K Expanded Experimental Results

### K.1 Open-Ended Generation Tasks

To assess applicability beyond single-turn QA, we evaluate EDFL on two open-ended generation tasks: dialogue (Wizard-of-Wikipedia (Dinan et al., 2019)) and abstractive summarization (CNN/DailyMail (Hermann et al., 2015)). For dialogue, the skeleton removes Wikipedia grounding (context ablation); for summarization, it uses temperature scaling ( $\tau = 1.8$ ) as no external information source exists. Since these tasks lack ground-truth “correctness,” we measure fluency (perplexity of continuations), informativeness (ROUGE-L vs reference), and human preference (50 examples, 3 raters, pairwise comparison vs fixed-length baseline).

Results show EDFL reduces tokens by 21-31% on open-ended tasks while maintaining acceptable quality: perplexity increases by 5-7% (acceptable fluency degradation), ROUGE-L drops by 3% (modest informativeness loss), and humans prefer EDFL outputs 54-58% of the time (near-parity with fixed-length). The larger variance ( $\pm 6-9$  tokens vs  $\pm 2-3$  on QA) reflects diverse response lengths in open-ended generation. These results suggest EDFL generalizes beyond factual QA, though the information-sufficiency criterion becomes less well-defined without clear grounding sources. For truly open-ended creative tasks (story generation, brainstorming), where no skeleton baseline exists, our method’s applicability remains limited, which is an important scope constraint.

Table 19 provides a systematic comparison of Sequential-EDFL against prior stopping methods across key dimensions.

The gate reduces the HighLift+Incorrect rate by 41% (from 18.5% to 10.9%) with modest TPCA increase (+7.1 tokens) and overhead growth (+4%, Table 3), narrowing the sufficiency-correctness gap while preserving anytime-valid guarantees. Under a verification policy that checks all outputs, the gate reduces verifier-call rate from 100% to  $\sim 17\%$  (gate validates 83% of stops, requiring full verification only for remaining 17% plus non-stopped sequences), representing a practical systems benefit but *not* a formal guarantee.

## L Proofs

We provide formal proofs for the key theoretical results underlying our Sequential-EDFL framework, establishing the validity of optional skipping and

Table 19: Method comparison: formal guarantees and efficiency.

Method	Formal Guarantee	Anytime Valid	Skeleton-Free	Tokens Saved	Overhead (%)	Tuning Required
Fixed-length	✗	✗	✓	0	0%	None
Entropy threshold	✗	✗	✓	17	3%	$\tau_H$
Conformal stopping	✓	✗	✓	25	8%	Calibration set
SelfCheck	✗	✗	✓	32	22%	Temperature
E-Value	✓	✓	✗	37	16%	$\lambda, \mu$
<b>Sequential-EDFL</b>	✓	✓	✗	<b>61</b>	<b>12%</b>	<b>None*</b>

\*Skeleton construction required but parameters auto-tuned via mixture e-processes

\*\*Tokens Saved computed as average reduction vs. 150-token fixed-length baseline

Table 20: Open-ended tasks: dialogue (Wizard,  $n = 300$ ) and summarization (CNN/DM,  $n = 300$ ).

Task	TPCA	Perplexity	ROUGE-L	Human Pref
<i>Wizard-of-Wikipedia (dialogue)</i>				
Fixed-length (150 tok)	150.0	12.3	–	–
EDFL (context ablation)	118.4 ± 8.7	13.1	–	58%
<i>CNN/DailyMail (summarization)</i>				
Fixed-length (80 tok)	80.0	18.7	0.412	–
EDFL (temperature $\tau = 1.8$ )	72.3 ± 6.2	19.4	0.398	54%

adaptive reset mechanisms within our statistical testing framework.

*Proof.* The proof of Lemma 3.2 establishes that optional skipping preserves the supermartingale property essential for statistical validity. Because our gate only waits (never triggers sooner), it cannot inflate Type-I error; it only trades a few tokens for better correctness. Formally, optional stopping for nonnegative supermartingales plus the fact that the gate only *delays* stopping (never advancing) implies validity is unchanged. See, e.g., time-uniform concentration via e-processes (Howard et al., 2021a; Vovk and Wang, 2021b; Waudby-Smith and Ramdas, 2023). When  $\hat{s}_t = 1$  triggers skipping, we set  $X_t = 0$ , yielding  $\tilde{Z}_t = 0 - \hat{\mu}_{t-1} \leq 0$  since  $\hat{\mu}_{t-1} \geq 0$  (all  $X_i \geq 0$ ). For  $\lambda > 0$  and  $\tilde{Z}_t \leq 0$ , the conditional expectation  $\mathbb{E}[\exp(\lambda \tilde{Z}_t) | \mathcal{F}_{t-1}] = \exp(\lambda \tilde{Z}_t) \leq 1 \leq \exp\left(\frac{\lambda^2(\hat{v}_{t-1} + \eta)}{2(1-c\lambda)}\right)$  remains bounded by our penalty function. The e-process update  $\mathbb{E}[M_t | \mathcal{F}_{t-1}] = M_{t-1} \cdot \mathbb{E}[\exp(\lambda \tilde{Z}_t - \psi_t(\lambda)) | \mathcal{F}_{t-1}] \leq M_{t-1}$  preserves the supermartingale property, and by optional stopping theorem (since  $\hat{s}_t \in \mathcal{F}_{t-1}$ ), Theorem 3.1 continues to hold.  $\square$

The proof of Theorem 3.3 extends validity to adaptive segment budgeting by defining segment-wise e-processes  $M_t^{(j)} = \sum_k w_k \exp\left(\lambda_k \sum_{i \in [t_j, t]} \tilde{Z}_i - \sum_{i \in [t_j, t]} \psi_i(\lambda_k)\right)$  where each segment  $j$  satisfies  $\mathbb{P}\left(\sup_t M_t^{(j)} \geq 1/\delta_j\right) \leq \delta_j$  by Theorem 3.1. Within segment  $j$ , apply Theorem 3.1 with budget

$\delta_j$ . Union bound over segments yields  $\sum_j \delta_j = \delta$ . Since  $\delta_j$  decays as  $j^{-2}$ , the series converges. This is a standard convergent-series budget allocation; cf. segment-wise testing with e-processes (Howard et al., 2021a; Ramdas et al., 2023). The union bound over segments yields  $\mathbb{P}\left(\exists j, t : M_t^{(j)} \geq 1/\delta_j\right) \leq \sum_{j=1}^{\infty} \delta_j = \sum_{j=1}^{\infty} \frac{6\delta}{\pi^2 j^2} = \delta$ , completing the proof that adaptive resets maintain overall error control at level  $\delta$ .

## M Computational Overhead Breakdown

Detailed profiling of Sequential-EDFL reveals that the 12.1% computational overhead stems primarily from skeleton logit computation, which dominates at 6.5% of baseline generation time. The remaining components contribute modestly: e-process computation across 12  $\lambda$  values adds 2.1%, drift estimation contributes 1.2%, information lift calculation requires 1.0%, entropy-slope computation adds 0.8%, and EMA updates consume 0.6%. This breakdown suggests optimization opportunities through skeleton caching or distilled models for the dominant component. Per-token latency analysis for streaming deployments appears in Appendix W.

## N Error Categorization

Analysis of Sequential-EDFL’s error patterns reveals well-calibrated behavior consistent with our theoretical framework. Early stopping (false positive) rates range from 6.1% (ProofWriter) to 11.4% (LegalBench), aligning closely with our target

$\delta = 0.10$  after accounting for conservative inflation. Late stopping (false negative) rates remain low at 2.9-6.3%, while timeout events occur rarely at 1.4-2.4%. The higher early stopping rates on complex datasets like LegalBench reflect appropriate conservatism in challenging domains where information accumulation patterns prove more variable.

## O Algorithmic Specification

This algorithm provides a complete, executable specification of Sequential-EDFL, integrating self-normalized e-processes (lines 13-17), mixture combination (line 18), anytime-valid stopping (lines 20-22), and adaptive drift handling (lines 24-28). The computational complexity is  $O(K)$  per token for  $K$  parameters, achieving 12% overhead with  $K = 12$  in our experiments.

Table 21: Overhead breakdown per 100 tokens (LLaMA-2-7B, A100, 1000 runs).

Component	Time (ms)	% of baseline
Baseline generation	$520 \pm 18$	–
Skeleton logits	$34 \pm 4$	6.5%
Lift $X_t$	$5 \pm 1$	1.0%
EMA updates ( $\hat{\mu}, \hat{v}$ )	$3 \pm 1$	0.6%
E-process (12 $\lambda$ s)	$11 \pm 2$	2.1%
Entropy-slope	$4 \pm 1$	0.8%
Drift estimator	$6 \pm 1$	1.2%
<b>Total overhead</b>	<b><math>63 \pm 6</math></b>	<b>12.1%</b>

---

**Algorithm 1** Sequential-EDFL algorithm with optional correctness gate.

---

**Require:** Input  $x$ , error rate  $\delta$ , skeleton model  $S$ , parameter grid  $\{\lambda_1, \dots, \lambda_K\}$

```
1: Initialize: segment  $J \leftarrow 1$ ,  $M_t(\lambda_k) \leftarrow 1$  for all  $k$ ,  $\hat{\mu} \leftarrow 0$ ,  $\hat{v} \leftarrow 0$ ,  $\alpha \leftarrow 0.1$ 
2: Set budget  $\delta_J \leftarrow 6\delta/(\pi^2 J^2)$ , threshold  $u_J \leftarrow 1/\delta_J$ 
3: for  $t = 1, 2, \dots$  do
4:   Sample  $y_t \sim P(\cdot|x, y_{1:t-1})$  from full model
5:   Compute skeleton probability  $s_t \leftarrow S(y_t|x, y_{1:t-1})$ 
6:   Compute full probability  $p_t \leftarrow P(y_t|x, y_{1:t-1})$ 
7:   Compute lift:  $X_t \leftarrow \log(p_t/s_t)$  ▷ Bounded to  $[0, c]$  via clipping
8:   // Optional Skipping
9:   if entropy slope  $H_{t-1} - H_{t-2} \geq 0$  then continue ▷ Skip high-uncertainty steps
10:  end if
11:  // Update EMA Estimates
12:   $\hat{\mu} \leftarrow (1 - \alpha)\hat{\mu} + \alpha X_t$ 
13:   $\hat{v} \leftarrow (1 - \alpha)\hat{v} + \alpha(X_t - \hat{\mu})^2 + \eta$  ▷  $\eta$ : inflation for conservatism
14:  // Update E-Processes for Each Parameter
15:  for  $k = 1, \dots, K$  do
16:     $M_t(\lambda_k) \leftarrow M_{t-1}(\lambda_k) \cdot \exp\left(\lambda_k(X_t - \hat{\mu}) - \frac{\lambda_k^2 \hat{v}}{2}\right)$ 
17:  end for
18:  // Mixture E-Process
19:   $M_t \leftarrow \sum_{k=1}^K w_k M_t(\lambda_k)$  where  $w_k = 1/K$  ▷ Uniform mixture
20:  // Stopping Decision
21:  if  $M_t \geq u_J$  then
22:    // Optional gate: only DELAYS stopping; never advances it (Lemma 3.2)
23:    if  $\text{IsSentenceBoundary}(y_{1:t})$  and  $\text{VerifierPass}(x, y_{1:t}) \geq \tau_c$  then
24:      return  $y_{1:t}$  ▷ Stop: info sufficient & gate passed
25:    else
26:      continue ▷ Delay stopping until boundary+verifier pass
27:    end if
28:  end if
29:  // Drift Detection
30:  Compute drift statistic  $\hat{d}_t \leftarrow |\hat{\mu}_{\text{recent}} - \hat{\mu}_{\text{overall}}|$ 
31:  if  $\hat{d}_t > \tau_d$  then
32:     $J \leftarrow J + 1$ , reset  $M_t(\lambda_k) \leftarrow 1$  for all  $k$ 
33:    Update budget  $\delta_J \leftarrow 6\delta/(\pi^2 J^2)$ , threshold  $u_J \leftarrow 1/\delta_J$ 
34:  end if
35: end for
```

---

## P Reproducibility Checklist

Our experiments ensure full reproducibility through systematic control of randomness and computational environment. Random seeds are fixed across all frameworks: NumPy uses seed 42, PyTorch uses seed 123, and Python’s random module uses seed 789. CUDA operations employ deterministic mode via `torch.use_deterministic_algorithms` to eliminate non-deterministic GPU computations. All datasets include SHA-256 checksums provided in supplementary material for integrity verification.

The experimental setup employs three language models: LLaMA-2-7B (`meta-llama/Llama-2-7b-hf`), LLaMA-2-13B (`meta-llama/Llama-2-13b-hf`), and GPT-4 (`gpt-4-0613`). Retrieval-augmented generation experiments use Contriever-MS MARCO with top-5 retrieval and maximum 512 tokens per document. The computational environment consists of 4xA100 (40GB) GPUs running CUDA 11.8 and PyTorch 2.0.1. All hyperparameters are comprehensively documented in Table 7, and complete source code will be released upon acceptance to ensure full experimental replication.

## Q Extended Related Work

Sequential-EDFL builds upon sequential testing theory, particularly e-processes (Vovk and Wang, 2021a; Ramdas et al., 2023; Howard et al., 2021a) that provide anytime-valid inference with roots in Ville’s martingale theory (Ville, 1939) and modern confidence sequences (Robbins, 1970; Lai, 1976; Howard et al., 2021b). Self-normalized e-processes (Howard et al., 2021a; Waudby-Smith and Ramdas, 2023) handle unknown centering via running variance estimation, directly inspiring our empirical-Bernstein extension. Recent work on sequential inference in LLMs (Lew et al., 2023) demonstrates the value of adaptive stopping, though without anytime-valid guarantees. Safe testing (Grünwald et al., 2019) and betting scores (Waudby-Smith and Ramdas, 2021) provide additional theoretical grounding and baseline comparisons for our anytime-valid framework.

Conformal prediction represents a complementary approach to uncertainty quantification that offers finite-sample guarantees through split conformal methods (Vovk et al., 2005; Angelopoulos and Bates, 2021), though requiring calibration sets. Extensions encompass conformalized quantile regres-

sion (Romano et al., 2019), distribution-free inference (Lei et al., 2018), and covariate shift adaptation (Tibshirani et al., 2019), with online variants (Gibbs and Candes, 2021) and time series extensions (Chen and Xie, 2020) addressing distribution shift. However, these approaches don’t naturally accommodate token-level stopping decisions in sequential generation, motivating our e-process framework.

Within the LLM uncertainty landscape, existing approaches include entropy-based methods (Malinin and Gales, 2018), semantic consistency checks (Manakul et al., 2023), verbalized confidence (Kadavath et al., 2022), and hallucination detection (Varshney et al., 2023; Band et al., 2024), yet these lack the formal statistical guarantees that our framework provides through frequentist control with anytime-valid error rates. Risk-aware decoding encompasses constrained generation (Hokamp and Liu, 2017), calibration techniques (Guo et al., 2017; Minderer et al., 2021; Kumar et al., 2019), and selective abstention (Geifman and El-Yaniv, 2017) using static thresholds, alongside out-of-distribution detection (Hendrycks and Gimpel, 2017; Liang et al., 2018; Lee et al., 2018) for uncertainty estimation. Our work extends this paradigm by providing sequential, anytime-valid control that dynamically adapts to evidence accumulation patterns.

Information-theoretic metrics in NLP (Meister et al., 2021; Sachan et al., 2021) inform our lift construction, though prior work lacks the statistical testing frameworks necessary for principled stopping decisions with formal guarantees. Recent advances in reasoning (Wei et al., 2022; Kojima et al., 2022; Wang et al., 2023), tool use (Schick et al., 2023; Yao et al., 2022; Chen et al., 2022), and retrieval-augmented generation (Lewis et al., 2020; Karpukhin et al., 2020; Borgeaud et al., 2022) demonstrate both the importance of controlled generation and the need for measuring information gain from external sources, directly motivating our skeleton-based approach to quantifying evidence accumulation.

Table 22: Error distribution for Sequential-EDFL ( $\delta = 0.1$ ) across datasets.

Dataset	Correct	Early (FP)	Late (FN)	Timeout
GSM8K	87.9%	7.3%	3.2%	1.6%
HotpotQA	82.7%	9.4%	5.6%	2.3%
ASQA	81.2%	10.3%	6.1%	2.4%
TruthfulQA	85.8%	8.1%	4.4%	1.7%
ProofWriter	89.6%	6.1%	2.9%	1.4%
LegalBench	79.9%	11.4%	6.3%	2.4%

Table 23: Economic value analysis: cost savings across deployment scenarios.

Scenario	Queries/day	$c_v$	$c_e$	Baseline Cost	EDFL Cost	Savings
Low-stakes QA	100K	\$0.001	\$0.00012	\$100	\$18.2	\$81.8 (82%)
Customer support	50K	\$0.01	\$0.0012	\$500	\$91	\$409 (82%)
Medical triage	10K	\$0.10	\$0.012	\$1,000	\$182	\$818 (82%)

## R Economic Value Analysis of Sufficiency Guarantees

This appendix provides formal cost modeling and economic analysis of deploying Sequential-EDFL in production systems. We model the total cost  $C_{\text{total}} = n \cdot (c_v \cdot p_v + c_e \cdot p_e)$  where  $n$  is the number of queries,  $c_v$  is the verification cost per query,  $c_e$  is the EDFL overhead cost per query,  $p_v$  is the verification rate (fraction of queries verified), and  $p_e$  is the EDFL application rate (1.0 for all queries). For uniform verification (baseline),  $p_v = 1.0$  and  $p_e = 0$ , yielding  $C_{\text{uniform}} = n \cdot c_v$ . For EDFL+selective verification,  $p_v < 1.0$  (filtered by EDFL) and  $p_e = 1.0$ , yielding  $C_{\text{EDFL}} = n \cdot (c_v \cdot p_v + c_e)$ . Break-even occurs when  $C_{\text{EDFL}} < C_{\text{uniform}}$ , i.e., when  $c_v \cdot p_v + c_e < c_v$ , which simplifies to  $p_v < 1 - c_e/c_v$ . For EDFL+Gate achieving  $p_v \approx 0.17$  (Table 3), this requires  $c_e/c_v < 0.83$ , meaning EDFL overhead must be less than 83% of verification cost.

Table 23 presents cost analysis across three deployment scenarios with varying query volumes and verification costs.

Assumptions: EDFL overhead  $c_e = 0.12 \times c_v$  (12% overhead), verification rate  $p_v = 0.17$  with gate (Table 3). Savings computed as  $(C_{\text{uniform}} - C_{\text{EDFL}})/C_{\text{uniform}} \times 100\%$ . EDFL+selective verification dominates uniform verification at equal budget by filtering low-lift sequences and allocating verification resources to high-uncertainty cases. At a fixed verification budget, EDFL achieves higher correctness rates by selectively verifying only the 17% of sequences flagged by the gate, compared to uniform verification of all sequences at the same total cost. For safety-critical applications, we recommend a cascade system: EDFL (filter)  $\rightarrow$  lightweight verifier (e.g., retrieval overlap, arith-

metic checker)  $\rightarrow$  expensive verifier (human review, domain expert). Empirical routing statistics and cost savings analysis appear in Appendix D.

## S LLM-as-Judge Sufficiency Validation

To validate our operational sufficiency definition without human annotation, we employ LLM-as-judge methodology using GPT-4o (gpt-4o-2024-08-06) as an automated evaluator, ensuring it was not used in training or calibration. For each stopped sequence, we prompt: “Given question  $Q$  and partial response  $R$  (truncated at token  $t$ ), is this response SUFFICIENT to answer the question? Respond with Yes or No. A response is sufficient if it contains the complete answer and requires no further tokens to address the question.” We evaluate on  $n = 500$  sequences per dataset (GSM8K, HotpotQA, ASQA), comparing EDFL stopping decisions with judge annotations. Table 24 reports agreement between EDFL sufficiency labels (answer-stability criterion) and LLM-as-judge annotations.

High agreement (82-87%) and moderate-to-substantial Cohen’s  $\kappa$  (0.64-0.74) validate that our answer-stability operationalization captures a meaningful sufficiency concept aligned with human-like judgment. Automated analysis of disagreements reveals two primary categories: (1) EDFL stops, Judge says insufficient (premature stops): 8-12% of cases, often due to partial numerical answers or incomplete reasoning chains; (2) EDFL continues, Judge says sufficient (conservative stops): 5-8% of cases, typically involving verbose explanations beyond minimal answers. We compare GPT-4o vs. Claude-3.5-Sonnet vs. Llama-3-70B-Instruct as judges on a subset ( $n = 200$  per

Table 24: LLM-as-judge agreement with EDFL sufficiency labels.

Dataset	Agreement	Judge Precision	Judge Recall	Cohen’s $\kappa$
GSM8K	87.2%	0.89	0.85	0.74
HotpotQA	84.6%	0.86	0.83	0.69
ASQA	82.1%	0.84	0.80	0.64

dataset). Inter-judge agreement ranges from 78-85% (GPT-4o vs. Claude-3.5) and 72-79% (GPT-4o vs. Llama-3-70B), indicating robust sufficiency concept across model families.

## T Alternative Sufficiency Definitions

This appendix validates our method’s robustness by evaluating  $\delta$ -control under alternative operational definitions of sufficiency, demonstrating that our approach is not overfitted to the answer-stability criterion. We evaluate four candidate sufficiency definitions: (1) **Answer-stability (baseline)**: Extracted answer at time  $t$  matches final answer  $A_T$ , and sequence is syntactically complete; (2) **Semantic-stability**: Cosine similarity between embeddings of  $y_{1:t}$  and  $y_{1:T}$  exceeds threshold  $\tau_{\text{sem}} = 0.95$  (using sentence-transformers/all-MiniLM-L6-v2); (3) **Perplexity-stability**: Perplexity of continuation  $P(y_{t+1:T}|y_{1:t}, x) < \tau_{\text{ppl}}$ , where  $\tau_{\text{ppl}}$  is calibrated on validation set; (4) **Information-theoretic**: Conditional entropy  $H(Y_{>t}|Y_{\leq t}, X) < \epsilon$ , computed via Monte Carlo sampling. Table 25 reports pairwise agreement between definitions on GSM8K ( $n = 500$ ).

Table 25: Cross-definition agreement for sufficiency labels (GSM8K,  $n = 500$ ).

Definition Pair	Agreement	Cohen’s $\kappa$
Answer vs. Semantic	91.4%	0.83
Answer vs. Perplexity	88.7%	0.77
Answer vs. Info-theoretic	85.2%	0.70
Semantic vs. Perplexity	89.3%	0.79

High agreement (85-91%) and substantial Cohen’s  $\kappa$  (0.70-0.83) indicate that alternative definitions capture similar sufficiency concepts, validating robustness of our operationalization. Table 26 reports empirical Type-I error rates under each definition with  $\delta = 0.1$  target.

All definitions yield controlled empirical risk (0.083-0.095, all below or near  $\delta = 0.1$ ) with similar TPCA (84-88 tokens), demonstrating that our method’s calibration properties are robust to the specific sufficiency operationalization. Since all definitions yield similar calibration and efficiency,

Table 26: Empirical risk ( $\delta = 0.1$  target) and TPCA under alternative sufficiency definitions (GSM8K).

Definition	Empirical Risk	TPCA
Answer-stability (baseline)	0.083 $\pm$ 0.010	84.3 $\pm$ 2.0
Semantic-stability	0.091 $\pm$ 0.011	86.7 $\pm$ 2.2
Perplexity-stability	0.089 $\pm$ 0.012	85.9 $\pm$ 2.1
Info-theoretic	0.095 $\pm$ 0.013	88.1 $\pm$ 2.3

we adopt answer-stability as the default due to its interpretability and alignment with end-user expectations (complete answers). Semantic-stability provides a viable alternative for tasks where answer extraction is ambiguous.

## U Code Generation Evaluation

Code generation offers clean sufficiency semantics (code runs or it doesn’t), enabling empirical validation of the sufficiency-correctness relationship. We evaluate on HumanEval (164 problems) and MBPP (374 problems). The skeleton uses context ablation: remove docstrings and example code, retaining only function signatures. Models: GPT-4 (gpt-4-0613), Llama-3-70B-Instruct, CodeLlama-34B-Instruct. For code generation, we define sufficiency as: (1) **Syntactic**: Code parses successfully (Python `ast.parse` succeeds); (2) **Functional**: Code passes all provided test cases; (3) **Complete**: No truncated statements or incomplete syntax. Table 29 reports TPCA, parse rate, Pass@1 (functional correctness), and  $\delta$ -control on HumanEval.

EDFL achieves 25-28% token reduction while maintaining parse rates and functional correctness comparable to fixed-length generation, with controlled empirical risk below  $\delta = 0.1$ . The correctness-sufficiency gap is smaller for code (8.2% for GPT-4) compared to QA tasks (13.2-22.7%), as high information lift better predicts functional correctness when code structure is well-defined. This validates that sufficiency operationalizations with verifiable ground truth (test case execution) yield tighter lift-correctness alignment.

## V Scaling and Robustness Analysis

This appendix evaluates EDFL’s performance across varying sample sizes, sequence lengths, and distribution shifts, demonstrating robustness of our calibration guarantees. Table 27 reports empirical risk across sample sizes on GSM8K.

Table 27: Sample size sensitivity: empirical risk ( $\delta = 0.1$  target) across sample sizes (GSM8K).

Sample Size $n$	Empirical Risk	95% CI
100	$0.092 \pm 0.029$	[0.063, 0.121]
250	$0.088 \pm 0.018$	[0.070, 0.106]
500 (default)	$0.083 \pm 0.010$	[0.073, 0.093]
1000	$0.081 \pm 0.007$	[0.074, 0.088]

Empirical risk remains controlled (below or near  $\delta = 0.1$ ) across all sample sizes, with tighter confidence intervals as  $n$  increases. Our default  $n = 500$  provides robust calibration estimates. Table 28 evaluates EDFL performance across maximum sequence lengths.

EDFL maintains controlled empirical risk (0.083-0.096) across sequence lengths, with adaptive resets preventing drift-induced degradation. Reset frequency increases with length (0.3 to 2.6 per sequence), but error control remains valid through convergent-series budget allocation. We evaluate zero-shot transfer: train skeleton diagnostics on Dataset A, test on Dataset B. Cross-dataset evaluation (GSM8K  $\rightarrow$  HotpotQA, HotpotQA  $\rightarrow$  ASQA) yields empirical risk 0.085-0.097 (all below  $\delta = 0.1$ ), confirming that skeleton diagnostics generalize across domains when information sources are similar (e.g., both RAG tasks). To assess graceful degradation, we intentionally miscalibrate skeletons: (1) Weak skeleton (KL  $< 2$ ): yields higher TPCA (95.2 vs. 84.3) but risk remains controlled (0.091); (2) Strong skeleton (KL  $> 10$ ): yields lower TPCA (78.6) but risk increases (0.106), approaching but not exceeding  $\delta = 0.1$  boundary. This validates that our diagnostics (KL  $\in [2, 10]$ ) are necessary for optimal efficiency while maintaining safety.

Table 28: Sequence length scaling: TPCA, empirical risk, and resets per sequence (GSM8K,  $n = 500$ ,  $\delta = 0.1$ ).

Max Length	TPCA	Emp Risk	Resets/Seq	Timeout Rate
150 (default)	$84.3 \pm 2.0$	$0.083 \pm 0.010$	0.3	1.6%
300	$92.1 \pm 2.4$	$0.089 \pm 0.011$	0.8	2.3%
500	$98.7 \pm 2.7$	$0.092 \pm 0.012$	1.4	3.1%
1000	$107.3 \pm 3.2$	$0.096 \pm 0.013$	2.6	4.8%

Table 29: Code generation results on HumanEval ( $n = 164$ ,  $\delta = 0.1$ ).

Model	Method	TPCA	Parse Rate	Pass@1	Emp Risk
GPT-4	Fixed-150	150.0	98.2%	87.8%	N/A
GPT-4	EDFL	$112.3 \pm 3.1$	97.6%	87.2%	$0.087 \pm 0.011$
Llama-3-70B	Fixed-150	150.0	94.5%	65.2%	N/A
Llama-3-70B	EDFL	$118.7 \pm 3.4$	94.1%	64.8%	$0.091 \pm 0.012$
CodeLlama-34B	Fixed-150	150.0	91.2%	48.8%	N/A
CodeLlama-34B	EDFL	$126.4 \pm 3.8$	90.8%	48.3%	$0.094 \pm 0.013$

## W Streaming Latency Analysis

This appendix provides detailed latency analysis for streaming deployment scenarios, addressing per-token latency and first-token latency impact. Table 30 reports per-token latency percentiles for LLaMA-2-7B on A100 GPU.

Table 30: Per-token latency breakdown (LLaMA-2-7B, A100, milliseconds).

Component	Mean	p50	p95	p99
Base decode	5.2	5.1	5.8	6.2
+ Skeleton logits	5.8	5.7	6.5	7.0
+ E-process update	5.9	5.8	6.6	7.1
+ Drift estimation	6.0	5.9	6.7	7.2

EDFL adds 0.8ms mean latency per token (15% relative increase), with p99 latency of 7.2ms remaining acceptable for interactive applications (target  $< 10$ ms). We evaluate skeleton computation every  $k$  tokens ( $k \in \{1, 2, 4, 8\}$ ). Lazy evaluation with  $k = 4$  reduces latency by 40% (5.5ms vs. 6.0ms) with minimal calibration impact (empirical risk 0.086 vs. 0.083), providing a practical optimization for latency-sensitive deployments. EDFL adds negligible overhead to time-to-first-token (0.2ms,  $< 5\%$  relative increase), as e-process initialization and skeleton setup occur before generation begins. This confirms suitability for interactive applications requiring low latency.